D.S.S. CONTRACT OST84-00125

"DETERMINATION OF STRESS INTENSITY FACTORS FOR WELD TOE DEFECTS" PHASE II

Final Report
(October 1985)

Prepared by:
R. Bell, P.Eng.

FACULTY OF ENGINEERING
CARLETON UNIVERSITY

Centre for Advanced Engineering & Design

Faculty of Engineering
Carleton University
Ottawa Canada K1S 5B6
Telephone (613)

DETERMINATION OF STRESS INTENSITY FACTOR FOR WELD TOE DEFECTS PHASE II

FINAL REPORT

BY

R. BELL P.ENG.

90pp

Work on this project was conducted under the auspices of Physical Metallurgy Research Laboratories Canada Centre for Mineral and Energy Technology,Energy, Mines and Resources Canada.

DSS FILE NUMBER: 22ST.23440-2-9083/1

DSS CONTRACT SERIAL NUMBER: 0ST84-00125

CANMET PROJECT NUMBER: 708801

CANMET SCIENTIFIC AUTHORITY: Dr. O. Vosikovsky

October 1985

This report should be cited by D.S.S. File No. 22ST.23440-2-9083/1

MICROMEDIA

ABSTRACT

This report describes finite element studies carried out to produce stress intensity factors for elliptical weld toe cracks in welded "T" plate specimens.

The stress intensity factors are utilized in a fatigue crack growth prediction program. This program is used to predict the fatigue propagation lives of "T" plate specimens with several thicknesses loaded in 3-point bending.

The predicted fatigue lives compare favourably with published experimental results.

RÉSUMÉ

Ce rapport décrit les études des éléments finis afin de déterminer les facteurs d'intensité de contraintes aux fissures ellipiques du fond de la soudure dans les spécimens soudés en feuilles "T".

Les facteurs d'intensité de contraintes sont utilisés dans une programme qui prédit la venue des fissures de fatigue. Cette programme est employées pour prédire les vies de propagation fatigue des spécimens soudés en feuilles "T", ayant les épaisseurs variantes, chargés au flexion trois pointes.

Les vies de fatigue prédites sont biens comparables avec les résultats experimentaux publiés.

TABLE OF CONTENTS

		Page
	ABSTRACT	
CHAPTER I	INTRODUCTION	3
1.1	Introduction	3
1.2	Conclusions of Phase I Report	4
1.3	Summary of Contents	6
1.4	Report of IWW Conference	7
CHAPTER II	3 - DIMENSIONAL STUDIES	9
2.1	Introduction	9
2.2	3-D Modelling of Semi-elliptical Weld Toe Cracks	9
2.3	3-D Weld Toe Cracks S.I.F. Results	10
2.4	Curve Fitting of Finite Element Results	12
CHAPTER III	FATIGUE CRACK GROWTH PREDICTION	38
3.1	Introduction	38
3.2	Computer Program	38
3.3	Prescribed Crack Shape	44
3.4	Life Prediction Results	47
3.4.1	Investigation of the Effect of Initial Crack Size	48
3.4.2	Crack Growth Curves	49
3.4.3	Influence of Thickness	49
CHAPTER IV	THE EFFECT OF SUPPORT SPAN ON S.I.F. RESULTS	73
4.1	Introduction	73
4.2	2-D Finite Element Results	74
4.3	Significance of Span Effect on Present Work	74
CHAPTER V	CONCLUSIONS	83
	REFERENCES	85
	APPENDIX A	87

ACKNOWLEDGEMENT

This work was performed for the Physical Metallurgy Research Laboratories, CANMET, Energy, Mines and Resources Canada under Supply and Services Canada Contract OST84-00125. The authors are indebted to PMRL CANMET for permission to publish this work. The authors also acknowledge the support and input received from Dr. O. Vosikovsky, PMRL in the Scientific administration of the contract.

DISCLAIMER

Any data presented, opinions, findings, conclusions, or recommendations expressed in this report are those of the authors and do not necessarily reflect the views of CANMET. Crown copyright of this report is reserved.

CHAPTER I

INTRODUCTION

1.1 Introduction

This report is the final report on D.S.S. Contract 0SU82-00233 and 0ST84-00125. The contract was divided into two phases; the work statements of which are identified and attached as Appendix A.

Phase I of the contract reviewed the literature regarding the application of fracture mechanics to the prediction of fatigue crack growth of weld toe cracks at tubular joints of offshore structures. Also included was a discussion on the use of the finite element method for the determination of fracture parameters and the numerical calculation of stress intensity factor (S.I.F.).

The general purpose finite element program ASAS was used to model a welded "T" plate specimen, Fig. 1.1 with a weld toe crack in 2 and 3 dimensions and the S.I.F. of the weld defect was calculated.

In the 2 - dimensional case stress intensity factors were presented for a series of straight fronted cracks with crack/thickness ratios, a/t, ranging from 0.005 to 0.7 for three different weld profiles. Empirical expressions were obtained from these results to describe the S.I.F. as a function of a/t.

In the 3 - dimensional studies the multi-level substructuring capabilities of ASAS were applied to investigate the variation of S.I.F. for semi-elliptical and semi-circular weld toe cracks. Crack tip stress intensity factors were presented for weld toe cracks having elliptical aspect ratios, a/c, of 1.0, 0.5, and 0.25 and depth/thickness ratios, a/t, in the range 0.05 to 0.4 for weld profiles of 30, 45 and 70.

For convenient reference the conclusions of Phase I of the contract are given below. (1)

1.2 Conclusions of Phase I Report

1. The work described in this report utilizes the finite element program ASAS together with a specially developed mesh generator to efficiently analyse the welded "T" specimens using linear elastic fracture mechanics.

2. The requirements of the original and the amended work statements have been met giving FE results for 2 - dimensional and 3-dimensional determination of the SIF at weld toe cracks.

3. Results using 2 - dimensional finite element analyses are presented for a range of weld toe cracks with crack depths between a/t = 0.005 and 0.7 and weld profiles of 30^{o}, 45^{o} and 70^{o}.

4. Empirical equations are fitted to the above 2 - dimensional SIF results. These equations agree with the FE results for the weld angles considered to within 2 - 3 percent, depending on the crack depth.

5. A stress analysis was performed on a series of uncracked "T" joints to obtain the stress distribution and the stress concentration factor SCF at the weld toe region. It was found from these analyses for the loading case of 3 - point bending that the distance of the support points from the weld toe has an effect on the SCF. For the cases considered this effect is quite small (5 - 13 percent); however further analyses should be performed to obtain the variation of SCF for a series of geometrically similar joints as the support distance is reduced.

6. Accuracy studies were performed on a semi-elliptical surface crack and an embedded crack in a cube subjected to tension. These analyses indicated that, for the best compromise between computing cost and accuracy, the mesh in the region of the crack should be constructed with a minimum of four crack tip elements around the crack, and the dimensions of these elements should be approximately $m/L = 2$ and $a/L = 5$.

7. The SIF for a series of crack shapes and crack depths for three different weld profiles are presented. In the main these results are for crack depths less than $a/t = 0.1$, which is the region indicated by the 2 - dimensional studies where the weld profile has the greatest effect on the SIF obtained.

8. The variation of SIF around semi-circular and semi-elliptical crack shapes of a/c = 1.0, 0.5 and 0.25 and crack depths, a/t varying between 0.025 and 0.4 are presented. The effect of crack shape, crack depth and weld angle on the SIF is demonstrated.

9. The versatility of the ASAS substructuring capability has been demonstrated in these studies. This program facility together with the aforementioned mesh generator for elliptical crack FE meshes permitted the 3 - dimensional studies to be carried out at reasonable cost.

1.3 Summary of Contents of this Report

The following report on Phase II of the contract presents studies carried out in accordance with the Technical Specification given in Appendix A.

Chapter II of this report describes further 3 - dimensional finite element studies carried out to supplement the Phase I data for the S.I.F. at an elliptical weld toe crack in a welded "T" plate specimen. An analytical curve fitting procedure for this data and a computer program to obtain the S.I.F. for a weld toe crack from the curve fitted data is also described.

Chapter III of the report describes the development and capabilities of a computer program for the prediction of the fatigue crack growth life of welded "T" joints using the S.I.F. data presented in chapter II.

This program has the capability to allow prescribed or natural crack shape development. Also included in this section are comparisons of fatigue crack depth against cycles, (a/N), with experimental data produced at PMRL for "T" plate joints. Finally, a series of S-N curves for "T" plate joints are presented showing the effect of initial crack size and plate thickness on the fatigue growth life.

Chapter IV describes a 2-dimensional finite element investigation to evaluate the effect of support span on the SIFs produced using FEM.

Chapter V presents conclusions for the work.

1.4 International Institute of Welding, (IIW) Conference

As required by the statement of work of the contract the author attended the IIW conference on Welding of Tubular Structures in Boston during July, 16 - 17, 1984.

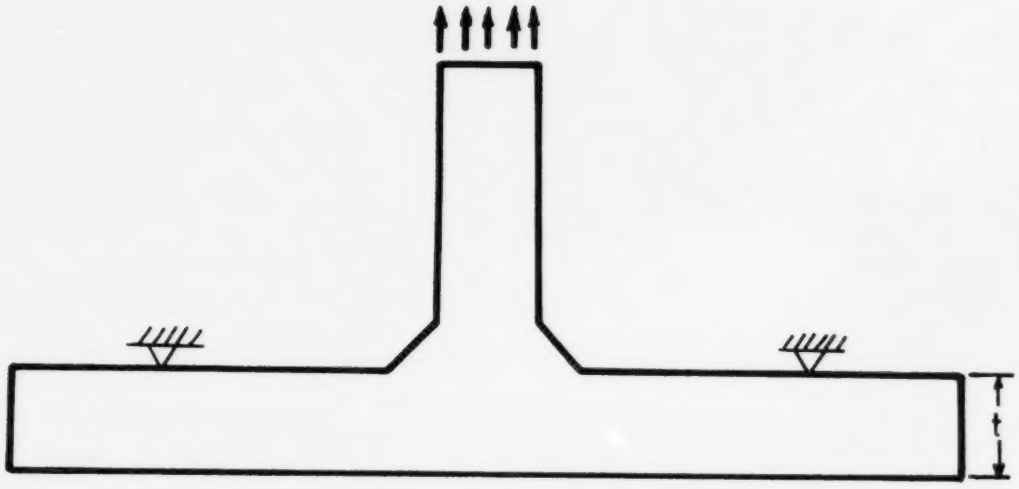

"T" SPECIMEN

FIG. 1·1

CHAPTER II

3 - DIMENSIONAL STUDIES

2.1 Introduction

This section of the report describes further 3 - dimensional finite element studies carried out to supplement the Phase I data for the stress intensity factor (S.I.F.) at an elliptical crack at the weld toe of a "T" plate specimen. Also described is an analytical curve fitting procedure for this data and a computer program to obtain the S.I.F. for the weld toe crack from the curve-fitted data.

2.2 3-D Modelling of Semi-Elliptical Weld Toe Cracks

The semi-elliptical weld toe crack in the "T" plate specimen was modelled and analysed using the finite element method as described in the Phase I report. The ASAS general purpose finite element program was again used and the finite element meshes were produced using a special purpose mesh generator which was developed at Carleton University. However, for the smaller a/t depth ratios the mesh generator had to be extensively modified.

The weld toe crack regior was modelled using the collapsed brick element, developed by Barsoum (2), which gives the required $1/\sqrt{r}$ singularity in the vicinity of the crack tip. The remainder of the "T" plate was modelled using 20 node isoparametric brick elements.

The substructuring techniques described in the Phase I report were also used in the analyses. The substructure representation of the "T" plate is shown in Fig. 2.1. It was possible in the substructure procedure to apply a series of loading and boundary conditions so that a series of different load cases could be analysed for each crack shape at the weld toe. The load cases considered were (i) axial tension, i.e., a non-load carrying weld, (ii) pure bending and (iii) three point bending, i.e., a load-carrying weld. Also analyses were performed for weld shapes of 30^{o}, 45^{o} and 70^{o}.

The physical dimensions of the model and the nomenclature of the crack shape are shown in Figs. 2.2 and 2.3 respectively. In each case the loading on the model was adjusted so that the axial stress σ_x at the weld toe had unit value.

2.3 3-D Weld Toe Crack S.I.F. Results

The 3-D weld toe crack cases considered in Phases I and II of this work are detailed in Table 2.1. In Phase II seven new crack shapes and depths were analysed. These cases were chosen after consultation with the scientific authority, so that the S.I.F. results could be obtained for smaller a/t ratios. This was necessary so that small initial crack sizes could be considered in the fatigue life prediction program, which will be described in a later section of this report. These Phase II cases are indicated in Table 2.1.

The finite element results for a weld angle of 45^{o} and the crack geometries and load cases examined are presented in Tables 2.2 and 2.3. In these tables the S.I.F. are presented as a magnification factor M_k which, when multiplied by the stress intensity factor for a surface crack in a flat plate, subjected to tension or bending loads as required, gives the stress intensity factor for the weld toe crack as shown below:

$$K_{I\ weld} = M_k \times K_{I\ surface\ crack}$$

The solution for $K_{I\ surface\ crack}$ was obtained from the empirical relationships of Newman and Raju (3).

In these tables $\theta = 0^{o}$ is the deepest point of the crack and $\theta = 90^{o}$ is the point where the crack intersects the surface of the plate, i.e., the weld toe. In the calculation of stress intensity factor plane strain conditions were assumed throughout except at the intersection of the crack with the plate surface, where plane stress conditions were assumed.

It should be noted that the stress intensity results at the crack-plate surface intersection should be used with caution because the finite element method models the crack region with a $r^{-\frac{1}{2}}$ singularity and it can be shown that the singularity at this surface re-entrant corner is of the form $r^{-\alpha}$, where α is less than 1/2 (4). Therefore the finite element results at this point are higher than they should be.

2.4 Curve Fitting of the Finite Element Results

In order that the stress intensity factor data can be utilized in a fatigue life prediction program it was necessary to fit curves to the data. However, it was not possible to fit simple expressions to the S.I.F. results because they vary with both crack shape, c/a and crack depth a/t.

Therefore a method utilizing bi-cubic spline functions was chosen to fit a surface to the variation of S.I.F. with a/t and c/a. The advantage of this method is that the entire domain of the surface can be represented by coefficients and to evaluate a S.I.F. one simply has to produce fundamental B-spline for the particular co-ordinates of the independent variables. These B-splines are then multiplied by the appropriate coefficients to produce the curve fitted value.

The bi-cubic spline coefficients were produced using the NAG library routine E02DAF which is available on the Carleton University mainframe computer. This routine takes the finite element S.I.F. data and produces bi-cubic spline coefficients which represents the surface which describes the variation of S.I.F. with a/t and c/a over the entire domain. The S.I.F. value of any value of a/t and c/a, which lie within the domain, can be evaluated using the above coefficients.

A series of B-spline coefficients were produced for the weld angles and load cases analysed, using the above library routine. These coefficients were installed in an evaluation program so that the S.I.F. could be calculated for any value of a/t and c/a.

Using the above procedure it is possible to reproduce the original finite element results to within several percentage points.

Tables 2.4 to 2.21 present the variation of S.I.F. with crack shape c/a and crack depth ratio a/t for a weld toe crack in a "T" plate joint with weld angles of 30^{o}, 45^{o} and 70^{o} loaded on tension, 4-point bending and 3-point bending. The results are presented for the deepest point and surface point of the crack, and were calculated using the above evaluation routine.

These results are presented as the magnification factor M_k as defined in section 2.3 and also as a non-dimensional parameter Y. In this case the stress intensity factor for the weld toe crack can be obtained by multiplying Y by the stress intensity for an embedded circular crack loaded in simple tension as shown below,

$$K_{I\ \text{weld}} = Y \times K_{I\ \text{circular crack}}$$

The solution for the embedded circular crack is obtained from

$$K_{I\ \text{circular}} = \sigma\sqrt{\pi a/Q}$$

where $Q \quad \pi^2/4$

TABLE 2.1

WELD TOE CRACK GEOMETRIES

a/c	a/t						
1.0	.005*	.01*	.025*	.05	.1	.2	.4
0.5	.005*	.0125*	.025	.05	.1	.2	
0.25	.005*		.025	.05	.1*		

* Phase II Data

a/t c/a	0.005	0.010	0.0125	0.025	0.050	0.100	0.200	0.400
1.0	3-pt=2.5701	tens=1.7130 4-pt=1.9533 3-pt=2.0597		tens=1.3405 4-pt=1.5201 3-pt=1.5345	tens=1.1936 4-pt=1.3152 3-pt=1.3461	tens=1.0204 4-pt=1.0563 3-pt=1.0578	tens=0.9299 4-pt=0.8897 3-pt=0.8836	tens=0.9399 4-pt=0.8288 3-pt=0.8237
2.0	3-pt=2.6137		tens=1.6217 4-pt=1.8924 3-pt=1.9238	tens=1.3646 4-pt=1.5699 3-pt=1.5992	tens=1.1420 4-pt=1.2735 3-pt=1.2869	tens=0.9904 4-pt=1.0486 3-pt=1.0566	tens=0.9475 4-pt=0.9359 3-pt=0.9355	
4.0	3-pt=2.6753			tens=1.3827 4-pt=1.5889 3-pt=1.6130	tens=1.1675 4-pt=1.2950 3-pt=1.3138	tens=1.0241 4-pt=1.0815 3-pt=1.0869		

TABLE 2.2 - Table of M_K for $\theta = 0^o$, for weld shape angle of 45^o

a/t c/a	0.005	0.010	0.0125	0.025	0.050	0.100	0.200	0.400
1.0	3-pt=3.8007	tens=2.6215 4-pt=3.0782 3-pt=3.1956		tens=2.1223 4-pt=2.4806 3-pt=2.5583	tens=1.8017 4-pt=2.1127 3-pt=2.1581	tens=1.3571 4-pt=1.5803 3-pt=1.6115	tens=1.1904 4-pt=1.4036 3-pt=1.4270	tens=1.0215 4-pt=1.0900 3-pt=1.0900
2.0	3-pt=3.4233		tens=2.7916 4-pt=3.2883 3-pt=3.3811	tens=2.1586 4-pt=2.5375 3-pt=2.6019	tens=1.7175 4-pt=2.0085 3-pt=2.0606	tens=1.4051 4-pt=1.6347 3-pt=1.6666	tens=1.1119 4-pt=1.1315 3-pt=1.1328	
4.0	3-pt=3.9721			tens=2.2088 4-pt=2.6000 3-pt=2.6569	tens=1.7815 4-pt=2.0723 3-pt=2.1133	tens=1.4805 4-pt=1.6985 3-pt=1.7342		

TABLE 2.3 - Table M_K for $\theta = 90^o$, for weld shape angle of 45^o

TABLE 2.4

S.I.F. FOR A WELDED 'T' PLATE SPECIMEN
LOADED IN TENSION, WITH A
70 DEGREE WELD PROFILE.
S.I.F. AT THE DEEPEST POINT OF THE CRACK.

Mk

a/t	c/a				
	1.0	1.5	2.0	3.0	4.0
.025	1.32650	1.22341	1.33359	1.34690	1.35420
.030	1.27804	1.16165	1.26120	1.26950	1.27828
.035	1.23875	1.11419	1.20733	1.21471	1.22370
.040	1.20670	1.07791	1.16780	1.17716	1.18545
.045	1.17994	1.04967	1.13838	1.15148	1.15851
.050	1.15653	1.02634	1.11490	1.13230	1.13787
.075	1.06124	.93760	1.02554	1.05716	1.05722
.100	.99551	.88481	.97110	1.00560	1.00309
.150	.93051	.85257	.93385	.95367	.95173
.200	.91710	.86064	.93681	.93741	.93840
.250	.91637	.85491	.92801	.92503	.92652
.300	.91140	.84084	.91301	.91391	.91460
.350	.90140	.83437	.90642	.90721	.90780
.400	.92800	.83375	.90142	.90211	.90260

Y

a/t	c/a				
	1.0	1.5	2.0	3.0	4.0
.025	1.380	1.554	1.876	2.091	2.199
.030	1.330	1.476	1.775	1.972	2.077
.035	1.290	1.416	1.700	1.888	1.990
.040	1.257	1.370	1.645	1.830	1.929
.045	1.229	1.335	1.604	1.792	1.886
.050	1.205	1.306	1.572	1.763	1.854
.075	1.108	1.196	1.450	1.653	1.732
.100	1.041	1.132	1.379	1.581	1.654
.150	.977	1.099	1.339	1.521	1.597
.200	.968	1.120	1.361	1.523	1.612
.250	.973	1.125	1.370	1.538	1.637
.300	.974	1.121	1.373	1.560	1.669
.350	.971	1.129	1.391	1.595	1.717
.400	1.008	1.146	1.414	1.636	1.775

TABLE 2.5

S.I.F. FOR A WELDED 'T' PLATE SPECIMEN
LOADED IN TENSION, WITH A
45 DEGREE WELD PROFILE.
S.I.F. AT THE DEEPEST POINT OF THE CRACK.

Mk

a/t	c/a				
	1.0	1.5	2.0	3.0	4.0
.010	1.70870	1.53199	1.69381	1.77473	1.76980
.015	1.56168	1.41731	1.55793	1.60794	1.60841
.020	1.44627	1.32379	1.44826	1.47684	1.48092
.025	1.35805	1.24869	1.36133	1.37650	1.38269
.030	1.29262	1.18922	1.29366	1.30200	1.30905
.050	1.17064	1.05258	1.14596	1.16380	1.16748
.075	1.09348	.95842	1.04820	1.08303	1.08188
.100	1.03326	.90139	.98820	1.02729	1.02409
.150	.95635	.86376	.94597	.97030	.96827
.200	.92543	.86977	.94824	.95159	.95270
.250	.92363	.86425	.93920	.93756	.93919
.300	.92446	.85095	.92384	.92519	.92600
.350	.91423	.84431	.91685	.91760	.91830
.400	.94001	.84283	.91096	.91179	.91240

Y

a/t	c/a				
	1.0	1.5	2.0	3.0	4.0
.010	1.777	1.944	2.381	2.752	2.871
.015	1.624	1.799	2.190	2.494	2.610
.020	1.505	1.681	2.037	2.292	2.404
.025	1.413	1.586	1.915	2.137	2.246
.030	1.345	1.511	1.821	2.022	2.127
.050	1.220	1.339	1.616	1.812	1.903
.075	1.141	1.222	1.482	1.693	1.772
.100	1.080	1.153	1.403	1.615	1.688
.150	1.004	1.113	1.357	1.547	1.625
.200	.977	1.132	1.378	1.546	1.636
.250	.981	1.137	1.387	1.559	1.659
.300	.988	1.135	1.389	1.579	1.690
.350	.985	1.142	1.407	1.613	1.737
.400	1.021	1.158	1.429	1.654	1.794

TABLE 2.6

S.I.F. FOR A WELDED 'T' PLATE SPECIMEN
LOADED IN TENSION, WITH A
30 DEGREE WELD PROFILE.
S.I.F. AT THE DEEPEST POINT OF THE CRACK.

Mk

a/t	c/a				
	1.0	1.5	2.0	3.0	4.0
.025	1.35020	1.24644	1.35691	1.36591	1.37080
.030	1.31108	1.18577	1.28859	1.30107	1.30515
.035	1.27771	1.14008	1.23797	1.25358	1.25703
.040	1.24898	1.10597	1.20100	1.21939	1.22236
.045	1.22377	1.08005	1.17360	1.19445	1.19705
.050	1.20098	1.05894	1.15172	1.17472	1.17702
.075	1.10669	.97654	1.06630	1.09602	1.09724
.100	1.03999	.92339	1.01059	1.04140	1.04211
.150	.96919	.87938	.96242	.98472	.98547
.200	.94820	.87596	.95549	.96530	.96650
.250	.94182	.87171	.94796	.95099	.95212
.300	.93570	.86332	.93749	.93860	.93940
.350	.92830	.85641	.92990	.93080	.93150
.400	.94860	.85432	.92409	.92499	.92560

Y

a/t	c/a				
	1.0	1.5	2.0	3.0	4.0
.025	1.405	1.583	1.909	2.121	2.226
.030	1.365	1.506	1.814	2.021	2.121
.035	1.330	1.449	1.743	1.948	2.044
.040	1.301	1.406	1.692	1.896	1.989
.045	1.275	1.374	1.654	1.859	1.949
.050	1.251	1.347	1.624	1.829	1.918
.075	1.155	1.245	1.508	1.714	1.797
.100	1.087	1.181	1.435	1.637	1.718
.150	1.018	1.133	1.380	1.570	1.654
.200	1.001	1.140	1.389	1.569	1.660
.250	1.000	1.147	1.400	1.581	1.682
.300	1.000	1.151	1.410	1.602	1.714
.350	1.000	1.159	1.427	1.636	1.762
.400	1.030	1.174	1.449	1.678	1.820

TABLE 2.7

S.I.F. FOR A WELDED 'T' PLATE SPECIMEN
LOADED IN 4-POINT BENDING, WITH A
70 DEGREE WELD PROFILE.
S.I.F. AT THE DEEPEST POINT OF THE CRACK.

Mk

a/t	c/a				
	1.0	1.5	2.0	3.0	4.0
.025	1.58940	1.46710	1.59790	1.61079	1.62080
.030	1.51727	1.36886	1.49039	1.51071	1.50595
.035	1.45586	1.29406	1.40903	1.43457	1.42301
.040	1.40309	1.23748	1.34796	1.37691	1.36441
.045	1.35688	1.19393	1.30130	1.33230	1.32259
.050	1.31516	1.15819	1.26320	1.29529	1.29000
.075	1.14291	1.02088	1.11571	1.14568	1.15722
.100	1.02149	.93581	1.02220	1.04100	1.05960
.150	.89323	.86982	.94422	.93006	.94409
.200	.85460	.85514	.92341	.88970	.89200
.250	.84064	.81261	.87936	.86043	.85999
.300	.82980	.76687	.83350	.83570	.83730
.350	.81480	.75276	.81800	.81990	.82130
.400	.80220	.74193	.80630	.80800	.80920

Y

a/t	c/a				
	1.0	1.5	2.0	3.0	4.0
.025	1.599	1.803	2.177	2.423	2.551
.030	1.516	1.672	2.018	2.259	2.357
.035	1.445	1.570	1.896	2.133	2.214
.040	1.383	1.492	1.803	2.035	2.111
.045	1.328	1.431	1.730	1.958	2.035
.050	1.279	1.379	1.669	1.892	1.974
.075	1.073	1.178	1.430	1.627	1.723
.100	.925	1.046	1.272	1.439	1.538
.150	.751	.911	1.108	1.220	1.306
.200	.662	.839	1.022	1.111	1.181
.250	.597	.745	.919	1.025	1.095
.300	.535	.656	.822	.953	1.028
.350	.472	.599	.761	.895	.974
.400	.412	.547	.707	.846	.930

TABLE 2.8

S.I.F. FOR A WELDED 'T' PLATE SPECIMEN
LOADED IN 4-POINT BENDING, WITH A
45 DEGREE WELD PROFILE.
S.I.F. AT THE DEEPEST POINT OF THE CRACK.

Mk

a/t	c/a				
	1.0	1.5	2.0	3.0	4.0
.010	1.94840	1.97941	1.98280	1.98693	2.12120
.015	1.78009	1.80571	1.81330	1.82150	1.89892
.020	1.64563	1.66547	1.67547	1.68724	1.72366
.025	1.54037	1.55423	1.56513	1.57999	1.58889
.030	1.45965	1.46749	1.47809	1.49557	1.48813
.050	1.28907	1.27591	1.27927	1.30299	1.29499
.075	1.16574	1.14160	1.13819	1.16172	1.17258
.100	1.07016	1.05014	1.04546	1.06240	1.08150
.150	.94656	.95851	.96084	.95604	.97102
.200	.88699	.92650	.93691	.91670	.91890
.250	.86272	.89411	.90330	.88895	.88736
.300	.85528	.85934	.86191	.86430	.86590
.350	.84876	.83474	.83275	.84603	.85087
.400	.82725	.83284	.83584	.83740	.83860

Y

a/t	c/a				
	1.0	1.5	2.0	3.0	4.0
.010	1.999	2.479	2.751	3.043	3.398
.015	1.814	2.247	2.501	2.773	3.024
.020	1.666	2.060	2.296	2.553	2.729
.025	1.549	1.910	2.132	2.377	2.501
.030	1.458	1.792	2.001	2.236	2.329
.050	1.253	1.519	1.690	1.904	1.981
.075	1.095	1.317	1.459	1.650	1.746
.100	.970	1.173	1.301	1.468	1.570
.150	.795	1.004	1.127	1.254	1.343
.200	.687	.909	1.037	1.145	1.217
.250	.612	.820	.944	1.059	1.129
.300	.551	.735	.850	.985	1.063
.350	.492	.664	.775	.924	1.009
.400	.425	.614	.733	.877	.964

TABLE 2.9

S.I.F. FOR A WELDED 'T' PLATE SPECIMEN
LOADED IN 4-POINT BENDING, WITH A
30 DEGREE WELD PROFILE.
S.I.F. AT THE DEEPEST POINT OF THE CRACK.

Mk

a/t	c/a				
	1.0	1.5	2.0	3.0	4.0
.025	1.47360	1.36926	1.48581	1.48119	1.47850
.030	1.43205	1.28787	1.40394	1.42667	1.41109
.035	1.39389	1.22907	1.34343	1.38094	1.36025
.040	1.35866	1.18753	1.29933	1.34225	1.32212
.045	1.32594	1.15794	1.26667	1.30882	1.29283
.050	1.29529	1.13498	1.24050	1.27889	1.26852
.075	1.16596	1.04329	1.13551	1.15543	1.16633
.100	1.07140	.97853	1.06190	1.06800	1.08819
.150	.96186	.90665	.98184	.97250	.98823
.200	.91730	.87289	.94640	.93500	.93709
.250	.89530	.84085	.91304	.90841	.90734
.300	.88140	.81418	.88471	.88671	.88810
.350	.86790	.80140	.87070	.87250	.87370
.400	.84620	.79043	.86021	.86171	.86280

Y

a/t	c/a				
	1.0	1.5	2.0	3.0	4.0
.025	1.482	1.683	2.024	2.228	2.327
.030	1.431	1.573	1.901	2.133	2.208
.035	1.383	1.491	1.808	2.053	2.117
.040	1.339	1.432	1.738	1.984	2.046
.045	1.298	1.387	1.684	1.923	1.989
.050	1.259	1.351	1.639	1.868	1.941
.075	1.095	1.203	1.456	1.641	1.737
.100	.971	1.093	1.321	1.476	1.579
.150	.808	.950	1.152	1.275	1.367
.200	.711	.856	1.048	1.167	1.241
.250	.636	.771	.954	1.083	1.155
.300	.568	.697	.873	1.011	1.090
.350	.503	.638	.811	.953	1.037
.400	.435	.582	.755	.902	.992

TABLE 2.10

S.I.F. FOR A WELDED 'T' PLATE SPECIMEN
LOADED IN 3-POINT BENDING, WITH A
70 DEGREE WELD PROFILE.
S.I.F. AT THE DEEPEST POINT OF THE CRACK.

Mk

a/t	c/a				
	1.0	1.5	2.0	3.0	4.0
.025	1.62240	1.49498	1.62917	1.64551	1.65810
.030	1.54026	1.39512	1.51921	1.53870	1.53596
.035	1.47236	1.31844	1.43542	1.45771	1.44783
.040	1.41573	1.25985	1.37195	1.39666	1.38566
.045	1.36743	1.21422	1.32299	1.34965	1.34138
.050	1.32450	1.17648	1.28272	1.31080	1.30694
.075	1.14704	1.03130	1.12673	1.15391	1.16677
.100	1.02080	.94150	1.02810	1.04420	1.06391
.150	.88504	.87210	.94638	.92808	.94268
.200	.84340	.85642	.92450	.88600	.88840
.250	.83159	.81038	.87683	.85545	.85495
.300	.82340	.76110	.82730	.82960	.83120
.350	.80780	.74635	.81110	.81310	.81460
.400	.79650	.73529	.79890	.80070	.80190

Y

a/t	c/a				
	1.0	1.5	2.0	3.0	4.0
.025	1.632	1.837	2.219	2.475	2.610
.030	1.539	1.704	2.057	2.301	2.404
.035	1.461	1.600	1.932	2.167	2.253
.040	1.395	1.519	1.835	2.064	2.144
.045	1.339	1.455	1.759	1.983	2.064
.050	1.288	1.401	1.695	1.915	2.000
.075	1.077	1.190	1.445	1.639	1.738
.100	.925	1.052	1.279	1.443	1.544
.150	.744	.914	1.110	1.217	1.304
.200	.654	.840	1.024	1.106	1.177
.250	.590	.743	.916	1.020	1.088
.300	.531	.651	.816	.946	1.020
.350	.468	.594	.755	.888	.966
.400	.409	.542	.701	.839	.922

TABLE 2.11

S.I.F. FOR A WELDED 'T' PLATE SPECIMEN
LOADED IN 3-POINT BENDING, WITH A
45 DEGREE WELD PROFILE.
S.I.F. AT THE DEEPEST POINT OF THE CRACK.

Mk

a/t	c/a				
	1.0	1.5	2.0	3.0	4.0
.005	2.49710	2.64744	2.54816	2.20444	2.67330
.010	2.16175	2.25394	2.19907	2.00820	2.30921
.015	1.89672	1.94399	1.92201	1.84580	2.01918
.020	1.69321	1.70717	1.70807	1.71329	1.79410
.025	1.54246	1.53306	1.54836	1.60669	1.62483
.050	1.27243	1.23852	1.25171	1.32359	1.29652
.075	1.18694	1.16615	1.16078	1.17455	1.18476
.100	1.10528	1.09965	1.08795	1.06959	1.09669
.150	.96452	.98792	.98597	.95671	.97809
.200	.87221	.91067	.92456	.91450	.91372
.250	.84091	.87104	.88512	.88479	.87927
.300	.84506	.85539	.85951	.85860	.86122
.350	.84961	.84590	.84224	.83920	.84876
.400	.81948	.82475	.82780	.82990	.83108

Y

a/t	c/a				
	1.0	1.5	2.0	3.0	4.0
.005	2.579	3.337	3.558	3.396	4.308
.010	2.218	2.823	3.051	3.075	3.699
.015	1.933	2.419	2.651	2.810	3.215
.020	1.714	2.111	2.341	2.592	2.840
.025	1.551	1.884	2.109	2.417	2.557
.050	1.237	1.475	1.654	1.934	1.984
.075	1.115	1.345	1.488	1.668	1.764
.100	1.001	1.229	1.354	1.478	1.592
.150	.810	1.035	1.157	1.255	1.353
.200	.676	.893	1.024	1.142	1.210
.250	.597	.799	.925	1.054	1.119
.300	.545	.732	.848	.979	1.057
.350	.492	.673	.784	.916	1.007
.400	.421	.608	.726	.869	.955

TABLE 2.12

S.I.F. FOR A WELDED 'T' PLATE SPECIMEN
LOADED IN 3-POINT BENDING, WITH A
30 DEGREE WELD PROFILE.
S.I.F. AT THE DEEPEST POINT OF THE CRACK.

Mk

a/t	c/a				
	1.0	1.5	2.0	3.0	4.0
.025	1.49700	1.38477	1.50388	1.50487	1.50790
.030	1.45346	1.30192	1.42039	1.44817	1.43567
.035	1.41359	1.24205	1.35863	1.40053	1.38132
.040	1.37690	1.19976	1.31354	1.36015	1.34068
.045	1.34288	1.16962	1.28008	1.32522	1.30957
.050	1.31104	1.14621	1.25320	1.29390	1.28384
.075	1.17637	1.05224	1.14502	1.16474	1.17593
.100	1.07743	.98516	1.06860	1.07330	1.09372
.150	.96181	.90890	.98408	.97348	.98932
.200	.91431	.87195	.94569	.93429	.93640
.250	.89181	.83847	.91073	.90638	.90536
.300	.87810	.81129	.88159	.88360	.88510
.350	.86400	.79796	.86699	.86879	.87010
.400	.84160	.78640	.85591	.85751	.85870

Y

a/t	c/a				
	1.0	1.5	2.0	3.0	4.0
.025	1.506	1.702	2.049	2.264	2.373
.030	1.452	1.590	1.923	2.165	2.247
.035	1.403	1.507	1.828	2.082	2.149
.040	1.357	1.447	1.757	2.010	2.074
.045	1.315	1.401	1.702	1.947	2.015
.050	1.275	1.365	1.656	1.890	1.964
.075	1.105	1.214	1.468	1.654	1.751
.100	.976	1.101	1.330	1.483	1.587
.150	.808	.952	1.155	1.277	1.368
.200	.709	.855	1.047	1.167	1.240
.250	.633	.769	.952	1.080	1.152
.300	.566	.694	.870	1.007	1.086
.350	.501	.635	.807	.949	1.032
.400	.432	.580	.751	.898	.987

TABLE 2.13

S.I.F. FOR A WELDED 'T' PLATE SPECIMEN
LOADED IN TENSION, WITH A
70 DEGREE WELD PROFILE.
S.I.F. AT THE SURFACE INTERSECTION OF THE CRACK.

M_k

a/t	c/a				
	1.0	1.5	2.0	3.0	4.0
.025	2.22840	1.99173	2.17217	2.22210	2.25600
.030	2.10432	1.83499	1.99875	2.05325	2.06153
.035	1.99914	1.72340	1.87475	1.92752	1.92985
.040	1.90934	1.64616	1.78838	1.83490	1.84543
.045	1.83140	1.59246	1.72782	1.76539	1.79269
.050	1.76181	1.55149	1.68130	1.70899	1.75609
.075	1.48547	1.38310	1.49053	1.47988	1.59500
.100	1.30749	1.25509	1.34680	1.31571	1.44983
.150	1.15748	1.09024	1.16523	1.13065	1.21291
.200	1.13339	.99703	1.06621	1.05081	1.05663
.250	1.09357	.92668	.99222	.99166	.98177
.300	1.04322	.87518	.93731	.94271	.94711
.350	1.01201	.84506	.90410	.90880	.91271
.400	.98070	.82053	.87798	.88220	.88588

Y

a/t	c/a				
	1.0	1.5	2.0	3.0	4.0
.025	2.551	2.272	2.377	2.191	2.016
.030	2.410	2.094	2.189	2.026	1.843
.035	2.290	1.968	2.054	1.903	1.727
.040	2.188	1.880	1.960	1.813	1.652
.045	2.100	1.820	1.895	1.746	1.607
.050	2.021	1.774	1.845	1.691	1.575
.075	1.708	1.587	1.643	1.472	1.439
.100	1.508	1.446	1.492	1.318	1.319
.150	1.346	1.271	1.309	1.153	1.127
.200	1.333	1.180	1.221	1.098	1.011
.250	1.303	1.117	1.162	1.068	.973
.300	1.262	1.078	1.128	1.051	.978
.350	1.246	1.067	1.121	1.054	.987
.400	1.231	1.064	1.126	1.068	1.007

TABLE 2.14

S.I.F. FOR A WELDED 'T' PLATE SPECIMEN
LOADED IN TENSION, WITH A
45 DEGREE WELD PROFILE.
S.I.F. AT THE SURFACE INTERSECTION OF THE CRACK.

Mk

a/t	c/a				
	1.0	1.5	2.0	3.0	4.0
.010	2.61420	2.74658	2.97314	2.86864	3.09800
.015	2.43294	2.42169	2.63090	2.59090	2.72085
.020	2.28016	2.16796	2.36213	2.36698	2.42846
.025	2.15230	1.97542	2.15663	2.18962	2.20882
.030	2.04581	1.83412	2.00415	2.05155	2.04991
.050	1.76244	1.58202	1.71988	1.74661	1.78152
.075	1.53379	1.43099	1.54189	1.52603	1.62199
.100	1.37906	1.31070	1.40377	1.36640	1.48051
.150	1.22806	1.14283	1.21962	1.18231	1.25365
.200	1.18275	1.03924	1.11237	1.09892	1.10493
.250	1.14049	.96691	1.03619	1.03772	1.03017
.300	1.09471	.91727	.98221	.98791	.99251
.350	1.05779	.88580	.94811	.95291	.95700
.400	1.02170	.85988	.92101	.92531	.92910

Y

a/t	c/a				
	1.0	1.5	2.0	3.0	4.0
.010	2.990	3.130	3.251	2.825	2.764
.015	2.784	2.761	2.877	2.553	2.429
.020	2.610	2.472	2.584	2.333	2.169
.025	2.464	2.254	2.360	2.159	1.974
.030	2.343	2.093	2.195	2.024	1.833
.050	2.022	1.809	1.888	1.729	1.598
.075	1.764	1.642	1.699	1.518	1.464
.100	1.591	1.510	1.555	1.368	1.347
.150	1.429	1.332	1.370	1.206	1.165
.200	1.391	1.230	1.273	1.149	1.057
.250	1.359	1.166	1.214	1.118	1.021
.300	1.324	1.130	1.182	1.102	1.025
.350	1.302	1.118	1.176	1.105	1.034
.400	1.282	1.115	1.181	1.120	1.056

TABLE 2.15

S.I.F. FOR A WELDED 'T' PLATE SPECIMEN
LOADED IN TENSION, WITH A
30 DEGREE WELD PROFILE.
S.I.F. AT THE SURFACE INTERSECTION OF THE CRACK.

Mk

a/t	c/a				
	1.0	1.5	2.0	3.0	4.0
.025	1.98350	1.80135	1.95913	1.98022	1.99660
.030	1.90585	1.69297	1.84352	1.87989	1.88062
.035	1.83701	1.61625	1.76026	1.80105	1.79958
.040	1.77563	1.56354	1.70158	1.73892	1.74484
.045	1.72038	1.52718	1.65974	1.68870	1.70777
.050	1.66991	1.49949	1.62699	1.64559	1.67974
.075	1.46765	1.38209	1.48886	1.46729	1.55319
.100	1.33552	1.28668	1.37929	1.33758	1.43823
.150	1.21809	1.14842	1.22711	1.18618	1.24843
.200	1.19044	1.05784	1.13289	1.11588	1.12090
.250	1.15212	.99258	1.06539	1.06448	1.05771
.300	1.10952	.94834	1.01840	1.02300	1.02688
.350	1.08281	.92222	.98960	.99370	.99709
.400	1.04040	.89902	.96692	.97051	.97370

Y

a/t	c/a				
	1.0	1.5	2.0	3.0	4.0
.025	2.271	2.055	2.144	1.953	1.784
.030	2.183	1.932	2.019	1.855	1.681
.035	2.105	1.845	1.928	1.778	1.610
.040	2.035	1.786	1.865	1.718	1.562
.045	1.973	1.745	1.821	1.670	1.530
.050	1.916	1.715	1.786	1.629	1.507
.075	1.688	1.586	1.641	1.460	1.402
.100	1.541	1.483	1.528	1.340	1.308
.150	1.417	1.339	1.379	1.210	1.160
.200	1.400	1.252	1.297	1.166	1.072
.250	1.373	1.196	1.248	1.146	1.048
.300	1.342	1.168	1.225	1.141	1.060
.350	1.333	1.164	1.227	1.153	1.078
.400	1.306	1.166	1.240	1.175	1.107

TABLE 2.16

S.I.F. FOR A WELDED 'T' PLATE SPECIMEN
LOADED IN 4-POINT BENDING, WITH A
70 DEGREE WELD PROFILE.
S.I.F. AT THE SURFACE INTERSECTION OF THE CRACK.

Mk

a/t	c/a				
	1.0	1.5	2.0	3.0	4.0
.025	2.88970	2.60379	2.83521	2.88243	2.92120
.030	2.74139	2.36288	2.57975	2.67000	2.65869
.035	2.60714	2.19874	2.40239	2.50643	2.47839
.040	2.48534	2.09233	2.28393	2.38062	2.36003
.045	2.37438	2.02463	2.20520	2.28150	2.28333
.050	2.27262	1.97659	2.14699	2.19800	2.22800
.075	1.87293	1.76233	1.89212	1.85461	1.98475
.100	1.62552	1.56732	1.67092	1.60601	1.76940
.150	1.43669	1.24875	1.32999	1.31902	1.42458
.200	1.40440	1.04827	1.12512	1.18870	1.19798
.250	1.29867	.97265	1.04213	1.09303	1.08215
.300	1.17660	.94600	1.00661	1.01520	1.02237
.350	1.12669	.89732	.95291	.96051	.96689
.400	1.07610	.85753	.91060	.91750	.92330

Y

a/t	c/a				
	1.0	1.5	2.0	3.0	4.0
.025	3.271	2.940	3.072	2.816	2.586
.030	3.097	2.663	2.791	2.605	2.351
.035	2.940	2.474	2.596	2.442	2.189
.040	2.797	2.351	2.464	2.317	2.082
.045	2.667	2.271	2.376	2.218	2.012
.050	2.548	2.214	2.310	2.134	1.962
.075	2.081	1.959	2.023	1.793	1.742
.100	1.791	1.732	1.778	1.548	1.550
.150	1.558	1.365	1.406	1.269	1.251
.200	1.503	1.138	1.186	1.149	1.062
.250	1.373	1.051	1.100	1.066	.974
.300	1.231	1.021	1.068	1.004	.939
.350	1.169	.969	1.018	.967	.911
.400	1.108	.928	.983	.943	.895

TABLE 2.17

S.I.F. FOR A WELDED 'T' PLATE SPECIMEN
LOADED IN 4-POINT BENDING, WITH A
45 DEGREE WELD PROFILE.
S.I.F. AT THE SURFACE INTERSECTION OF THE CRACK.

Mk

a/t	c/a				
	1.0	1.5	2.0	3.0	4.0
.010	3.06830	3.46302	3.51271	3.26595	3.70590
.015	2.85366	3.06320	3.09588	2.98636	3.23648
.020	2.67263	2.75109	2.77100	2.75668	2.87285
.025	2.52104	2.51433	2.52503	2.57030	2.60002
.030	2.39472	2.34052	2.34498	2.42061	2.40296
.050	2.05883	2.02719	2.02350	2.05679	2.07231
.075	1.79080	1.82413	1.81390	1.77041	1.87571
.100	1.61280	1.64712	1.62650	1.56120	1.69850
.150	1.44397	1.37076	1.32534	1.31497	1.40705
.200	1.38644	1.19716	1.13413	1.19941	1.20751
.250	1.30779	1.11737	1.05454	1.11598	1.10077
.300	1.20961	1.09023	1.03844	1.04682	1.05313
.350	1.12699	1.06659	1.02528	.99419	1.02219
.400	1.09500	.99726	.95450	.96041	.96560

Y

a/t	c/a				
	1.0	1.5	2.0	3.0	4.0
.010	3.494	3.930	3.825	3.205	3.294
.015	3.243	3.470	3.366	2.926	2.873
.020	3.031	3.111	3.008	2.697	2.547
.025	2.854	2.839	2.736	2.511	2.302
.030	2.706	2.638	2.537	2.362	2.125
.050	2.308	2.270	2.177	1.997	1.825
.075	1.990	2.028	1.940	1.711	1.646
.100	1.777	1.820	1.731	1.505	1.488
.150	1.566	1.499	1.401	1.266	1.236
.200	1.483	1.300	1.196	1.159	1.070
.250	1.383	1.208	1.113	1.089	.991
.300	1.266	1.176	1.101	1.036	.967
.350	1.169	1.152	1.096	1.001	.963
.400	1.127	1.080	1.030	.988	.936

TABLE 2.18

S.I.F. FOR A WELDED 'T' PLATE SPECIMEN
LOADED IN 4-POINT BENDING, WITH A
30 DEGREE WELD PROFILE.
S.I.F. AT THE SURFACE INTERSECTION OF THE CRACK.

Mk

a/t	c/a				
	1.0	1.5	2.0	3.0	4.0
.025	2.18520	1.98856	2.16191	2.18229	2.20280
.030	2.11509	1.84712	2.01838	2.08400	2.07971
.035	2.04671	1.75412	1.92084	2.00349	1.99265
.040	1.98074	1.69732	1.85780	1.93698	1.93272
.045	1.91788	1.66447	1.81776	1.88068	1.89103
.050	1.85880	1.64333	1.78922	1.83081	1.85871
.075	1.62631	1.54091	1.65705	1.62261	1.71192
.100	1.48318	1.43213	1.52970	1.47001	1.57851
.150	1.37433	1.22403	1.30756	1.28884	1.35770
.200	1.35088	1.07619	1.15900	1.20191	1.20803
.250	1.27638	1.02323	1.10209	1.13866	1.13169
.300	1.19403	1.00963	1.08252	1.08811	1.09281
.350	1.16143	.97747	1.04701	1.05201	1.05620
.400	1.11400	.94940	1.01898	1.02349	1.02740

Y

a/t	c/a				
	1.0	1.5	2.0	3.0	4.0
.025	2.474	2.245	2.343	2.132	1.950
.030	2.390	2.082	2.184	2.033	1.839
.035	2.308	1.974	2.075	1.952	1.760
.040	2.229	1.907	2.004	1.885	1.705
.045	2.154	1.867	1.958	1.828	1.667
.050	2.084	1.840	1.925	1.778	1.637
.075	1.807	1.713	1.772	1.568	1.502
.100	1.634	1.582	1.628	1.417	1.383
.150	1.491	1.338	1.382	1.240	1.192
.200	1.445	1.168	1.222	1.162	1.071
.250	1.349	1.106	1.163	1.111	1.018
.300	1.249	1.089	1.148	1.076	1.004
.350	1.205	1.055	1.119	1.059	.995
.400	1.147	1.028	1.100	1.052	.996

TABLE 2.19

S.I.F. FOR A WELDED 'T' PLATE SPECIMEN
LOADED IN 3-POINT BENDING, WITH A
70 DEGREE WELD PROFILE.
S.I.F. AT THE SURFACE INTERSECTION OF THE CRACK.

Mk

a/t	c/a				
	1.0	1.5	2.0	3.0	4.0
.025	2.98250	2.67310	2.91352	2.97499	3.02680
.030	2.82338	2.43227	2.65731	2.75494	2.74611
.035	2.68112	2.26725	2.47824	2.58502	2.55451
.040	2.55345	2.15923	2.35736	2.45388	2.42996
.045	2.43814	2.08943	2.27576	2.35019	2.35044
.050	2.33292	2.03907	2.21450	2.26259	2.29390
.075	1.91981	1.81312	1.94510	1.90204	2.04416
.100	1.66373	1.60697	1.71110	1.64079	1.81991
.150	1.46678	1.26928	1.35012	1.33861	1.45447
.200	1.43034	1.05645	1.13320	1.20089	1.21081
.250	1.31719	.97664	1.04583	1.09993	1.08759
.300	1.18822	.94902	1.00879	1.01789	1.02542
.350	1.13558	.89766	.95210	.96010	.96691
.400	1.07850	.85531	.90752	.91461	.92080

Y

a/t	c/a				
	1.0	1.5	2.0	3.0	4.0
.025	3.376	3.018	3.157	2.906	2.680
.030	3.190	2.741	2.875	2.688	2.428
.035	3.023	2.551	2.678	2.519	2.256
.040	2.874	2.426	2.543	2.388	2.144
.045	2.739	2.344	2.452	2.285	2.072
.050	2.616	2.284	2.383	2.197	2.020
.075	2.133	2.016	2.080	1.839	1.794
.100	1.833	1.775	1.821	1.581	1.595
.150	1.591	1.388	1.427	1.288	1.277
.200	1.530	1.147	1.195	1.161	1.073
.250	1.393	1.056	1.104	1.073	.979
.300	1.243	1.024	1.070	1.007	.942
.350	1.178	.969	1.017	.967	.911
.400	1.110	.926	.980	.940	.893

TABLE 2.20

S.I.F. FOR A WELDED 'T' PLATE SPECIMEN
LOADED IN 3-POINT BENDING, WITH A
45 DEGREE WELD PROFILE.
S.I.F. AT THE SURFACE INTERSECTION OF THE CRACK.

Mk

a/t	c/a				
	1.0	1.5	2.0	3.0	4.0
.005	3.70860	3.58886	3.54611	3.65769	3.97560
.010	3.32590	3.28630	3.27032	3.32437	3.51837
.015	3.01271	3.03248	3.03581	3.04622	3.15006
.020	2.76075	2.82174	2.83790	2.81680	2.85972
.025	2.56177	2.64846	2.67190	2.62971	2.63644
.050	2.07227	2.14600	2.15694	2.10450	2.14310
.075	1.83725	1.84794	1.83314	1.80593	1.91332
.100	1.67186	1.62544	1.59119	1.58749	1.71729
.150	1.48898	1.35356	1.29621	1.32954	1.41667
.200	1.40163	1.22316	1.15861	1.20769	1.22167
.250	1.31167	1.14301	1.08123	1.11981	1.11047
.300	1.21628	1.08576	1.03164	1.04719	1.05220
.350	1.13651	1.04002	.99358	.99194	1.01372
.400	1.09340	.99440	.95083	.95619	.96190

Y

a/t	c/a				
	1.0	1.5	2.0	3.0	4.0
.005	4.232	4.081	3.868	3.595	3.539
.010	3.787	3.730	3.561	3.262	3.128
.015	3.424	3.436	3.300	2.984	2.796
.020	3.131	3.191	3.080	2.756	2.535
.025	2.900	2.990	2.895	2.569	2.334
.050	2.324	2.403	2.321	2.043	1.887
.075	2.042	2.055	1.960	1.746	1.679
.100	1.842	1.796	1.693	1.530	1.505
.150	1.615	1.480	1.370	1.280	1.244
.200	1.500	1.328	1.222	1.167	1.083
.250	1.387	1.235	1.141	1.092	.999
.300	1.273	1.172	1.094	1.036	.967
.350	1.179	1.123	1.062	.999	.955
.400	1.125	1.076	1.026	.983	.932

TABLE 2.21

S.I.F. FOR A WELDED 'T' PLATE SPECIMEN
LOADED IN 3-POINT BENDING, WITH A
30 DEGREE WELD PROFILE.
S.I.F. AT THE SURFACE INTERSECTION OF THE CRACK.

Mk

a/t	c/a				
	1.0	1.5	2.0	3.0	4.0
.025	2.22240	2.02359	2.19990	2.21969	2.23840
.030	2.15699	1.88224	2.05650	2.12248	2.11173
.035	2.08940	1.78877	1.95850	2.04183	2.02285
.040	2.02139	1.73106	1.89455	1.97429	1.96237
.045	1.95475	1.69702	1.85330	1.91640	1.92093
.050	1.89125	1.67456	1.82341	1.86470	1.88916
.075	1.64194	1.56562	1.68444	1.64834	1.74305
.100	1.49062	1.45079	1.55062	1.48941	1.60699
.150	1.33179	1.23270	1.31740	1.29990	1.37529
.200	1.36437	1.07881	1.16179	1.20819	1.21460
.250	1.28767	1.02421	1.10270	1.14158	1.13360
.300	1.19990	1.01034	1.08260	1.08849	1.09348
.350	1.16562	.97646	1.04519	1.05049	1.05500
.400	1.11600	.94693	1.01570	1.02050	1.02460

Y

a/t	c/a				
	1.0	1.5	2.0	3.0	4.0
.025	2.516	2.285	2.384	2.168	1.982
.030	2.437	2.122	2.225	2.071	1.867
.035	2.356	2.013	2.116	1.989	1.787
.040	2.275	1.945	2.044	1.921	1.731
.045	2.196	1.904	1.997	1.863	1.693
.050	2.121	1.875	1.962	1.811	1.664
.075	1.825	1.741	1.801	1.593	1.530
.100	1.642	1.603	1.650	1.435	1.408
.150	1.499	1.348	1.393	1.251	1.208
.200	1.460	1.171	1.225	1.168	1.076
.250	1.361	1.107	1.164	1.114	1.020
.300	1.256	1.090	1.148	1.077	1.004
.350	1.209	1.054	1.117	1.058	.994
.400	1.149	1.025	1.096	1.049	.993

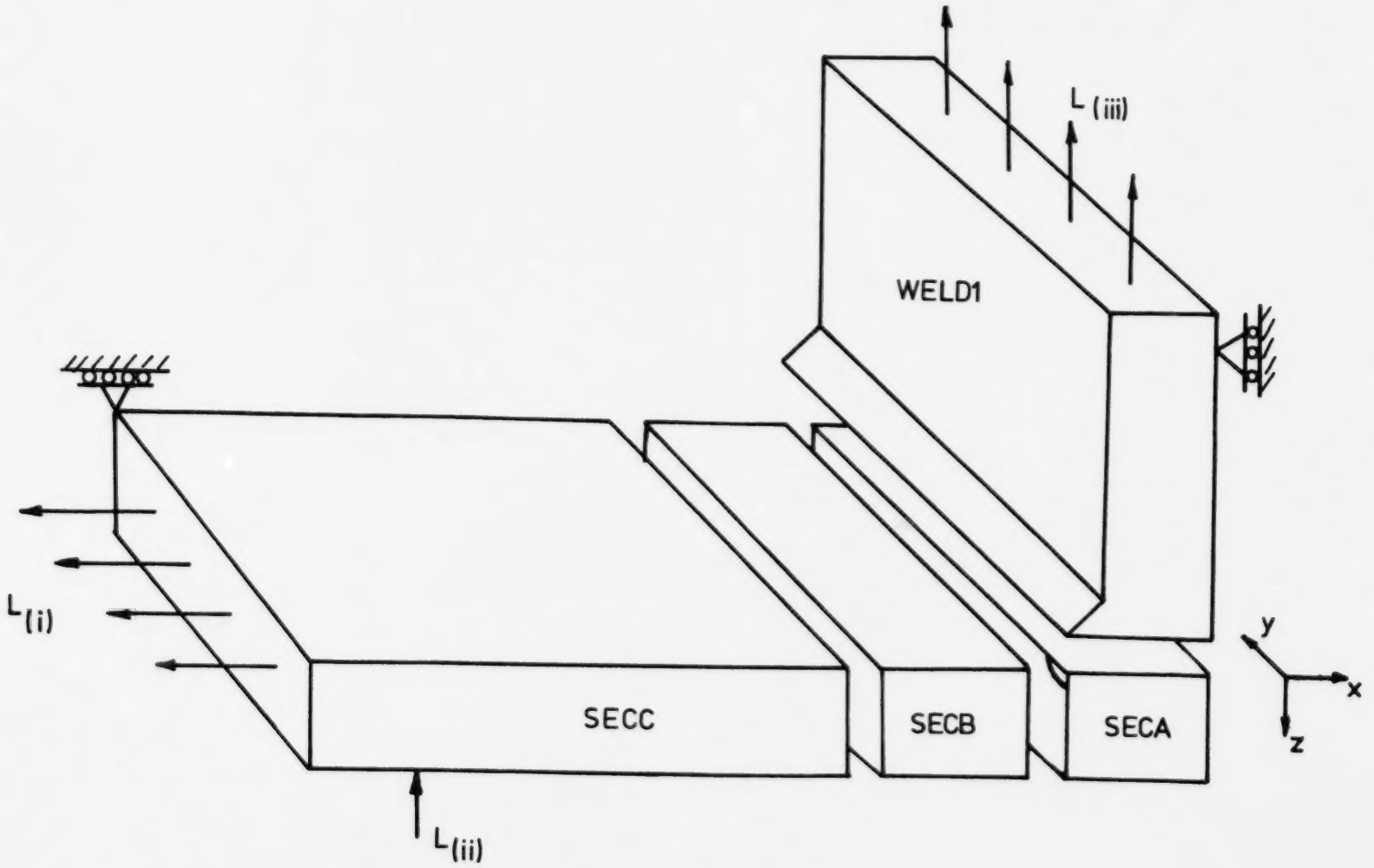

FIG. 2.1

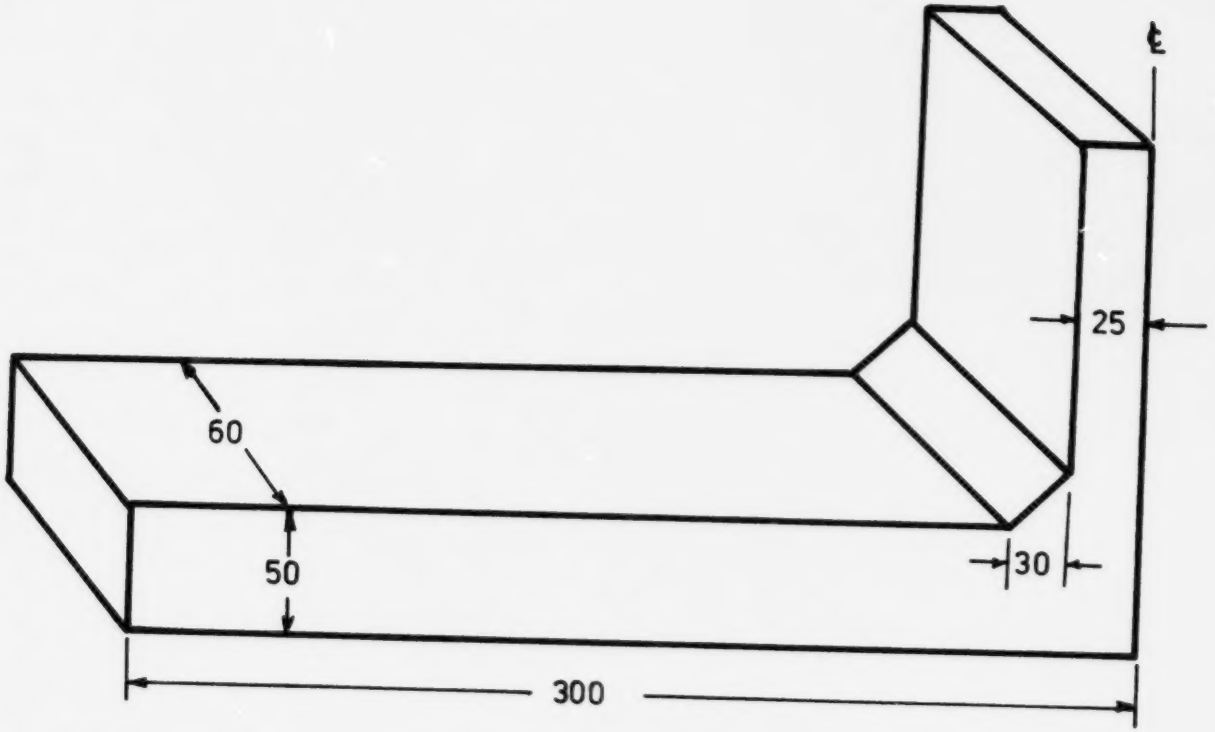

Dimension in mm

Dimensions of Finite Element Model

Figure 2.2

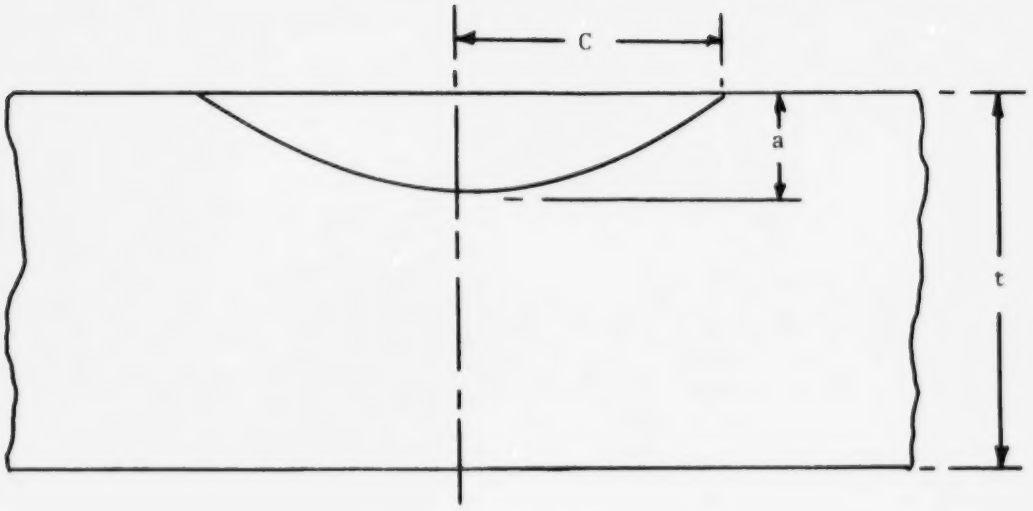

CRACK NOMENCLATURE

FIG. 2.3

CHAPTER III

FATIGUE CRACK GROWTH PREDICTION

3.1 Introduction

This chapter of the report describes a computer program which was written to predict the fatigue crack growth of an elliptical or straight fronted crack at the weld toe of a "T" plate specimen. This program is named FATCRACKS and uses the S.I.F. data described in the previous chapter. A method is described to utilize the development of the crack shape monitored during experimental tests to prescribe the crack shape development during crack growth calculations.

Results are presented comparing the predicted crack growth with experimental data obtained at PMRL using an A.C. potential crack monitoring system. Also presented are a series of S-N curves for "T" plate specimens showing the effect of initial crack size on the growth life of the plate joints.

3.2 Computer Program for Fatigue Crack Growth Prediction

Fatigue crack propagation can be described by a growth law such as for example the Paris Law

$$da/dN = C\Delta K^m \qquad (3.1)$$

where da/dN is the crack growth rate, C and m are material constants

and ΔK is the variation of stress intensity factor given by $K = Y \sigma \sqrt{\pi a}$. The stress intensity factor (SIF), K describes the stress environment at the crack tip and for two different geometries of the same material the stress distribution at the crack will be identical if the stress intensities are equal. It follows that the fatigue crack propagation in the two bodies will be identical if the variation in K is the same.

The life of a structure or component can be predicted by integration of the above equation as:

$$\int_0^N dN = \frac{1}{\pi^{m/2} C \Delta\sigma^m} \cdot \int_{a_i}^{a_f} \frac{da}{Y^m a^{m/2}} \qquad (3.2)$$

where a_i and a_f are the initial and final crack lengths respectively.

The computer program described herein is based on the above cycle by cycle integration and the growth laws are integrated using a Runge-Kutta numerical integration procedure.

The computer program requires the following initial input and has the capabilities listed below:

1. Initial Input.

   - initial crack depth a
   - initial crack length c
   - plate thickness
   - plate half width

- weld angle (30^{o}, 45^{o} or 70^{o})
- final crack depth
- weld toe stress range
- stress ratio
- material toughness K_{IC}
- fatigue crack propagation threshold K_{th}
- material growth law constants, C and m, for the a direction
- material growth law constants, C and m, for the c direction
- loading (tension, 4-point or 3-point bending)

2. Growth Law Selection

The program predicts fatigue crack growth according to the following growth laws:

(i) The Paris Law

$$da/dN = C\Delta K^{m} \tag{3.3}$$

where da/dN is the crack growth rate, C and m are material constants and ΔK is the variation in stress intensity factor at the crack tip.

(ii) The Forman Law

$$da/dN = C \frac{\Delta K^{m}}{(1-R)K_{c} - \Delta K} \tag{3.4}$$

where R is the stress ratio σ min/σ max and K_{c} is the fracture toughness of the material.

(iii) The Collipriest Law

$$da/dN = C\ (\Delta K_{th}\ K_c)^{m/2} \cdot EXP\left[\ell n\left(\frac{K_c}{\Delta K_{th}} \right)^{m/2} \text{arctanh} \right. \qquad (3.5)$$

$$\left. \ell n\ \frac{[\Delta K^2/\{(1-R)K_c\ \Delta K_{th}\}]}{\ell n[(1-R)K_c/\Delta K_{th}]} \right]$$

(iv) The Paris Law with Two Regions

In this option it is possible to select a value of K after which the Paris Law follows a different slope as shown in Fig. 3.1. This effect has been indicated by experimental results (5).

3. Stress Intensity Factor Evaluation

The program can evaluate K for straight fronted or semi-elliptical weld toe cracks according to the following relationships:

A. Straight Fronted Cracks

(i) Gurney and Johnston Equation (6).

This empirical equation was obtained from finite element analyses for non-load carrying fillet welds for welded joints with a wide range of weld sizes and plate thicknesses. The finite element analysis was carried out using a very large number of 2-dimensional constant strain triangular elements to model the joint.

(ii) Phase 1 2-Dimensional Expressions

These empirical expressions were obtained from the 2-dimensional finite element results presented in section 4.3 of the Phase I report.

The finite element analyses were performed using the collapsed isoparametric element which imposes the $1/\sqrt{r}$ singularity in the crack tip region.

B. Semi-Elliptical Surface Cracks

The stress intensity factor for a Semi-elliptical surface crack can be evaluated using one of the following empirical relationships.

(i) Newman and Raju Equations (3)

These empirical equations present an empirical stress intensity equation for a surface crack as a function of parametric angle, crack depth, crack length, plate thickness and plate width for tension and bending loads. The equation was developed from stress intensity factors obtained from 3-dimensional finite element analyses using singularity elements at the crack tip region of the model.

(ii) Phase II Empirical Expressions

Using this option the stress intensity factor of a crack at the weld toe of a "T" plate joint loaded in tension, 4-point or 3-point bending may be evaluated using the empirical equation described in section 2.4 of this report.

(iii) Irwin's Equation (7)

The stress intensity factor solution for an elliptical crack embedded in a plate of infinite depth and surface is also included in the program. This equation is of the following form:

$$K_I(\phi) = \frac{\sigma_o}{Q}\sqrt{\frac{\pi a}{c}} \cdot (a^2 \mathrm{Sin}^2\phi + c^2 \cos^2\phi)^{\frac{1}{4}} \qquad (3.6)$$

where Q is the elliptical integral of the 2nd kind, and σ_o is a uniform tensile stress.

4. Loading Conditions

As required by the work statement of the contract provision has been made in the program to permit constant or variable amplitude loading. The variable amplitude loading is performed using a block loading approach. It should be noted that the variable amplitude loading option has not been thoroughly tested.

5. Cycle Increment and Initiation Cycles

The crack growth is calculated in the a and c direction on a cycle by cycle basis. This option allows the user to specify the cycle interval at which crack growth will be printed. Also it is possible to specify a value of initiation cycles at which the program commences to calculate crack growth.

6. Natural or Prescribed Crack Shape Development

This option allows the user to specify the development of the crack shape during the growth calculations. If natural crack growth development is chosen the increase in crack length in the a and c directions is calculated by integration of the growth equation using the values of material parameters for the a and c values of crack length as the minor and major axes of the ellipse respectively. This procedure is assumed to represent the growth of a single elliptical crack.

If the prescribed crack shape development is chosen then the crack shape develops according to an imposed relationship. In this work the development of the prescribed crack shape development relationships are described in section 3.3. This prescribed crack shape development is assumed to describe the growth and coalescence of multiple weld toe cracks.

7. Changing from 3-D to 2-D Crack Growth

There is also included in the program the option of setting a value of crack shape ratio, a/c, at which the crack growth switches from 3-D to 2-D growth. At this point and on all following load cycles the calculation of ΔK is performed using one of the 2-D relationships for stress intensity factor.

3.3 Prescribed Crack Shape Development

As explained in the previous section the growth of a single semi-elliptical crack can be predicted by integrating the growth law on a cycle-by-cycle basis in the depth direction to obtain the change in crack depth, a, and in the surface direction to obtain the change in crack length, c. Using these values, a new elliptical crack shape is obtained. This procedure models the behaviour of a single elliptical crack and has been termed the single crack (SC) solution.

However, it has been found from an experimental study of "T" plate specimens loaded in 3-point bending (9) that there is a multi-nucleation of cracks along the length of the weld toe, and that the

number of cracks that initiate depends on the stress range and the plate thickness. These cracks tend to have initial crack shapes of a/c = 1.0; as they grow deeper the a/c value decreases and, eventually they coalesce and grow as a straight-fronted crack.

In order to characterize crack shape development as a function of stress range and plate thickness the aspect ratios of all cracks contained within the plate can be plotted as function of crack depth. This data for a test specimen thickness of 25 mm is shown in Fig. 3.2 (Ref. 9). If it is assumed that the initial small cracks are semi-circular the mean variation of crack aspect ratio can be described by the relationship

$$a/c = e^{-ka} \tag{3.7}$$

The parameter k in this equation which describes the variation of mean crack ratio with crack depth, was determined by fitting least square regression lines to ln a/c vs a plots for all test specimens. The dependence of k on plate thickness and stress range is shown in Figure 3.3 and Table 3.1.

To model this behaviour in the life prediction program, the following procedure was adopted. The initial crack shape a/c was chosen to be 1.0 and the crack growth in the depth direction was calculated in the normal way. However, the change in crack shape was prescribed by updating the length c, of the crack in the surface direction at each growth increment using the empirical relationships given in Table 3.1 . This procedure describes the development of a

mean crack shape and accomodates different crack growth rates in the depth and surface directions. In this work it has been termed the multiple crack solution (MC). For all predictions when the aspect ratio of the crack reached a value of 0.2, the crack was assumed to be straight-fronted and the procedure outlined in section 3.2, option 6 was followed.

3.4 Life Prediction Results

This section of the report presents fatigue life prediction results for welded "T" place specimens which were obtained using the computer program described in section 3.2.

The specimen geometries and dimensions are those described in reference (9) and are also shown in fig. 3.4. The experimental results cited for comparison are also taken from (9).

The specimens were loaded in 3-point bending, therefore the weld was load carrying. In the predicted results the initial crack shape was assumed to be semicircular, (a/c = 1.0), in all cases and the growth was changed from semi-elliptical crack growth to straight fronted crack growth at a/c = 0.2. In order to simulate multiple crack growth and crack coalescence the empirical crack growth equations described in section 3.3 and reference (9) were used.

In all cases the life of the specimen was assumed to have expired when the crack depth reached a depth of a/t = 0.5. It should be noted that in all the predicted results the life given is the propagation life i.e., there is no initiation life included.

The growth of the cracks were predicted using the Paris growth law and the material constants were chosen to be:

$$C = 5.36 \times 10^{-12}$$

$$m = 3.0$$

3.4.1 Investigation of Initial Crack Size

To investigate the effect of the initial crack size on the propagation life of the test specimens detailed in fig. 3.4, a series of computer runs were carried out on the five specimen thicknesses at five stress range levels of 75, 100, 150, 200 and 300 MPa.

In order to obtain the empirical crack shape development for the specimens at the 75 and 300 MPa stress ranges, the empirical equation derived using the 100, 150 and 200 MPa stress range experimental data was assumed to apply. This equation is given in (9) and is of the form

$$a/c = e^{-ka}$$

In this case the parameter k is given by

$$k = \frac{k_B}{(\Delta\sigma_B)^2 \, (t_B/t)^{\frac{1}{2}}} \, (\Delta\sigma)^2 \qquad (3\ 8)$$

where t_B is a reference thickness and $\Delta\sigma_B$ is the associated stress range, t is any thickness and $\Delta\sigma$ is its associated stress range. For the 300 MPa stress level predictions a reference thickness t_B = 26 mm and corresponding reference values of $\Delta\sigma_B$ = 116 MPa and k_B = 0.2 were chosen. For the 75 MPa stress level predictions the limiting value of k = 0.2 was chosen.

The results of the initial crack size investigation are given in tables 3.2 to 3.6 and are plotted on S-N diagrams in figs. 3.5 to 3.9, for the five plate thicknesses. Also shown in these plots are the experimental results (solid lines) of the propagation life of the specimens (9).

It can be seen that the predicted S-N curves are not straight lines, which is due to the fact that an empirical crack shape development based on the experimental results was imposed on the crack growth prediction.

3.4.2 a-N Prediction Results

Figures 3.10 to 3.14 show plots of a vs N for the analytical model compared with the experimental curves obtained using the AC crack monitoring system. It should be noted that the predicted results include only propagation life, while the experimental curves include both initiation and propagation life. The results for the 16 mm, 52 mm and 78 mm thicknesses are for an intial crack size of a_i = 0.3 mm while the results for the 26 mm thickness is for an initial crack size of a_i = 0.15 mm, and the results for the 103 mm thickness is for an initial crack size of a_i = 1.0 mm. These initial crack sizes were chosen to give a selection of results and do not reflect any attempt to give a best fit of predicted results as compared with experimental results.

It can be seen from these results that in some cases the predicted life is non-conservative depending on the initial crack depth chosen. However, in all cases the predicted results are within what would be considered as acceptable accuracy for fatigue investigation.

3.4.3 Influence of Thickness

Figures 3.15 to 3.17 show the data contained in Tables 3.2 to 3.6, plotted to demonstrate the effect of thickness on propagation life for fixed initial crack sizes of a_i = 0.3, 0.5 and 1.0 mm.

TABLE 3.1

EXPRESSIONS FOR k AS A FUNCTION OF PLATE THICKNESS

Stress Range	Expression
200 MPa	$k = 0.427 + .00863\ t$
150 MPa	$k = 0.193 + .00432\ t$
100 MPa	$k = 0.190 + .00074\ t$

TABLE 3.2

PROPAGATION LIFE TO $a_f = t/2$ FOR A "T" SPECIMEN

WITH t = 16 mm

FOR VARYING INITIAL CRACK SIZE

INITIAL CRACK SIZE a_i (mm)	LIFE (k CYCLES)				
	STRESS RANGE 75 MPa	STRESS RANGE 100 MPa	STRESS RANGE 150 MPa	STRESS RANGE 200 MPa	STRESS RANGE 300 MPa
0.08	20160	8150	1940	502	41
0.15	18960	7650	1799	446	38
0.20	18350	7400	1728	419	36
0.25	17820	7180	1666	395	34
0.30	17330	6980	1608	374	33
0.40	16400	6598	1500	335	31
0.50	15530	6230	1397	298	29
0.70	14000	5592	1218	238	26
1.00	12360	4910	1030	179	22
1.50	10510	4134	824	119	17
2.00	9120	3550	670	77	13

TABLE 3.3

PROPAGATION LIFE TO $a_f = t/2$ FOR A "T" SPECIMEN

WITH t = 26mm

FOR VARYING INITIAL CRACK SIZE

INITIAL CRACK SIZE a_i (mm)	LIFE (k CYCLES)				
	STRESS RANGE 75 MPa	STRESS RANGE 100 MPa	STRESS RANGE 150 MPa	STRESS RANGE 200 MPa	STRESS RANGE 300 MPa
.15	10440	4250	998	260	31.5
.2	10020	4080	948	241	30
.25	9700	3945	910	227	29.5
.3	9410	3830	876	216	28.5
.4	8920	3625	819	196	27
.5	8480	3440	768	179	26
.7	7650	3100	675	149	24
1.0	6560	2650	554	114	21
1.5	5255	2115	415	78	18
2.0	4390	1760	328	57	15

TABLE 3.4

PROPAGATION LIFE TO $a_f = t/2$ FOR A "T" SPECIMEN

WITH t = 52 mm

FOR VARYING INITIAL CRACK SIZE

INITIAL CRACK SIZE a_i (mm)	LIFE (k CYCLES)				
	STRESS RANGE 75 MPa	STRESS RANGE 100 MPa	STRESS RANGE 150 MPa	STRESS RANGE 200 MPa	STRESS RANGE 300 MPa
0.25	4944	1924	397	117	22
0.3	4766	1850	378	110	22
0.4	4492	1738	348	101	21
0.5	4277	1649	326	94	20
0.7	3934	1508	292	84	19
1.0	3514	1338	252	72	18
1.5	2908	1094	200	59	16
2.0	2398	893	159	50	15
2.5	2004	740	132	45	13

TABLE 3.5

PROPAGATION LIFE TO $a_f = t/2$ FOR A "T" SPECIMEN

WITH t = 78mm

FOR VARYING INITIAL CRACK SIZE

INITIAL CRACK SIZE a_i (mm)	LIFE (k CYCLES)				
	STRESS RANGE 75 MPa	STRESS RANGE 100 MPa	STRESS RANGE 150 MPa	STRESS RANGE 200 MPa	STRESS RANGE 300 MPa
0.3	3320	1245	255	83	19
0.4	3090	1151	232	75	17
0.5	2925	1086	217	71	17
0.7	2690	992	196	64	16
1.0	2430	890	173	57	15
1.5	2090	760	148	49	14
2.0	1805	656	128	46	13
2.5	1505	558	113	43	12

TABLE 3.6

PROPAGATION LIFE TO $a_f = t/2$ FOR A "T" SPECIMEN

WITH t = 103mm

FOR VARYING INITIAL CRACK SIZE

INITIAL CRACK SIZE a_i (mm)	LIFE (k CYCLES)				
	STRESS RANGE 75 MPa	STRESS RANGE 100 MPa	STRESS RANGE 150 MPa	STRESS RANGE 200 MPa	STRESS RANGE 300 MPa
0.5	2313	835	170	60	14
0.7	2111	755	153	54	13
1.0	1905	680	137	48	12
1.5	1664	590	119	44	11
2.0	1473	520	106	42	11
2.5	1307	460	97	39	10
3.0	1159	409	92	37	9

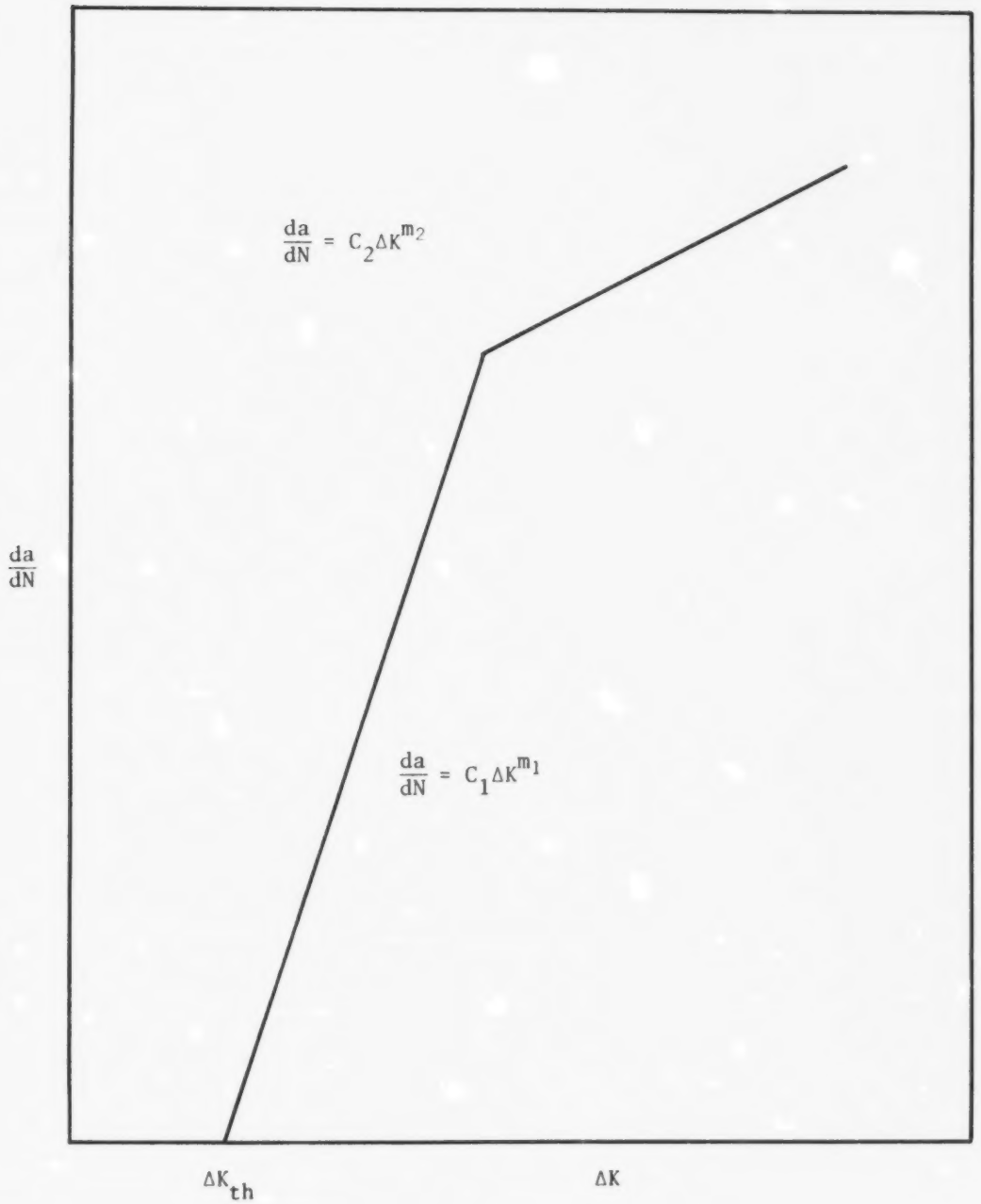

2 Region Paris Growth Law Option

Fig. 3.1

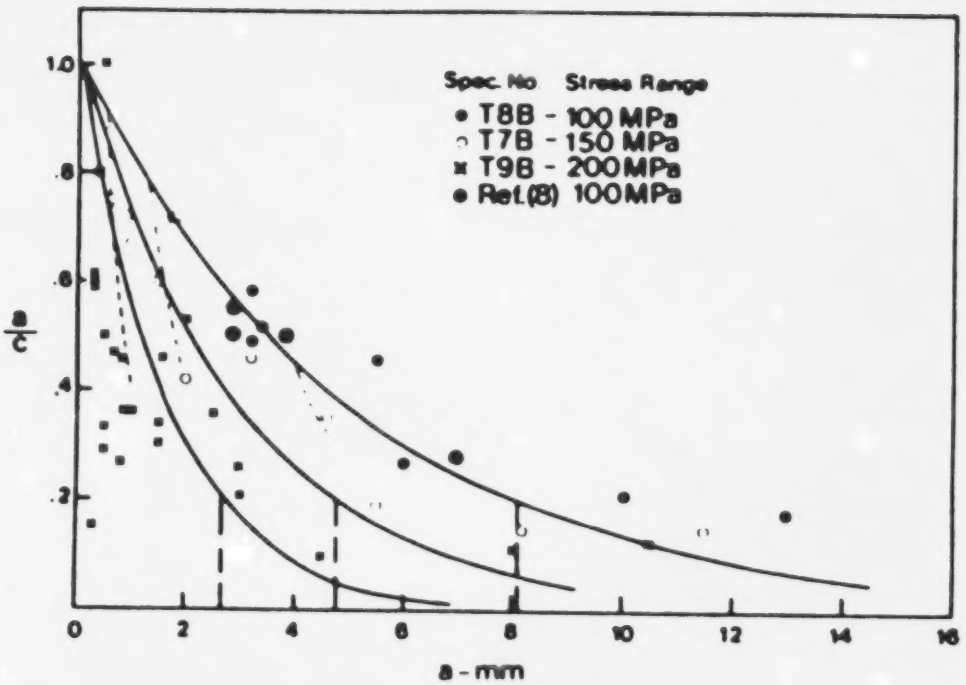

Fig. 3.2 - Measured aspect ratio variation with crack depth for t = 26 mm and $\Delta\sigma$ = 100, 150 and 200 MPa. The solid curves represent the mean aspect ratio variation given by Eq. 3.8. The dotted curves indicate the deviation from the single crack shape curve, resulting from coalescence of uniformly-distributed initial cracks.

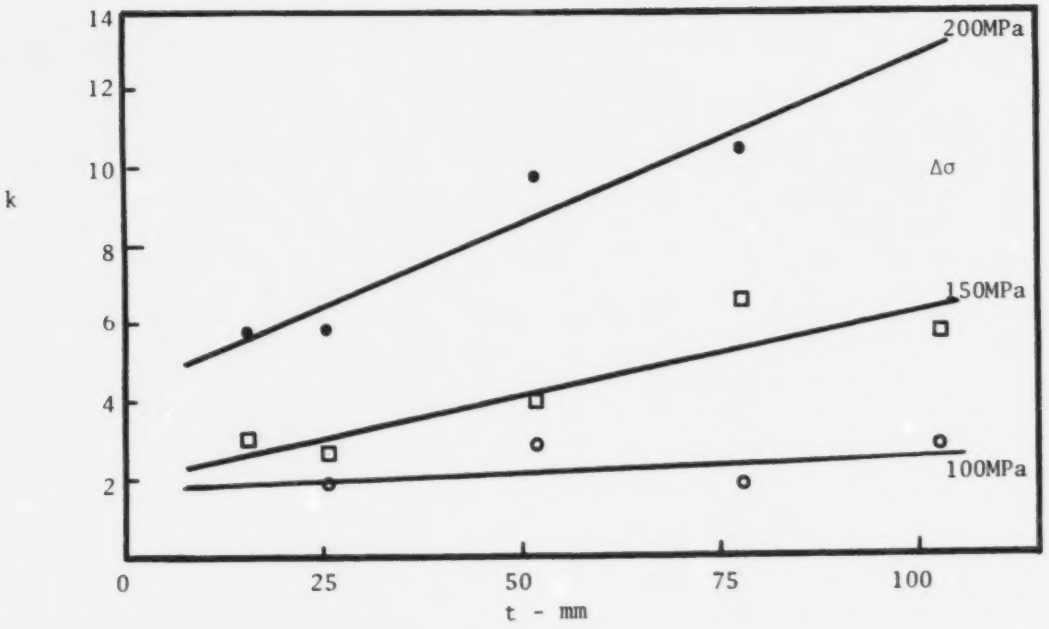

Fig. 3.3 - The dependence of parameter k in Eq. 3.7 on thickness.

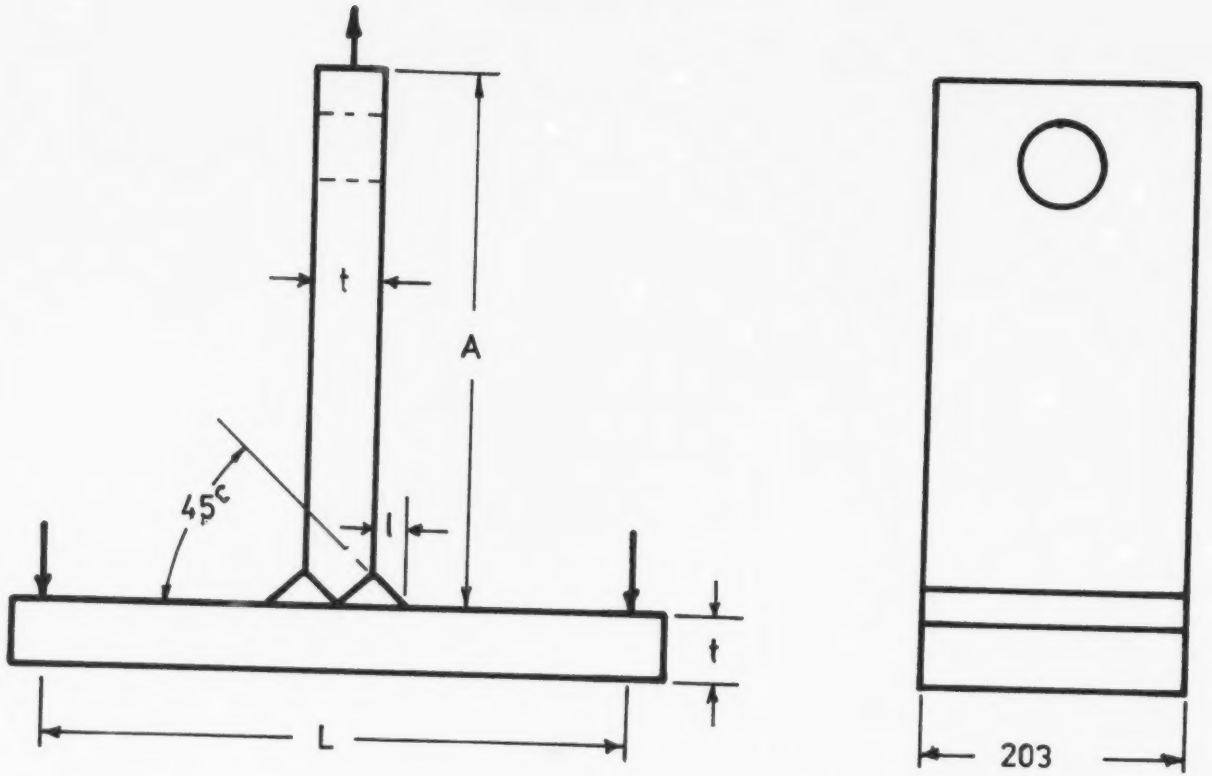

JOINT	T (mm)	ℓ (mm)	L (mm)	A (mm)
A	16	8-12	300	406
B	28	14-18	442	406
C	52	26-30	442	406
D	78	38-42	584	457
E	102	52-56	726	457

Specimen Geometries
Figure 3.4

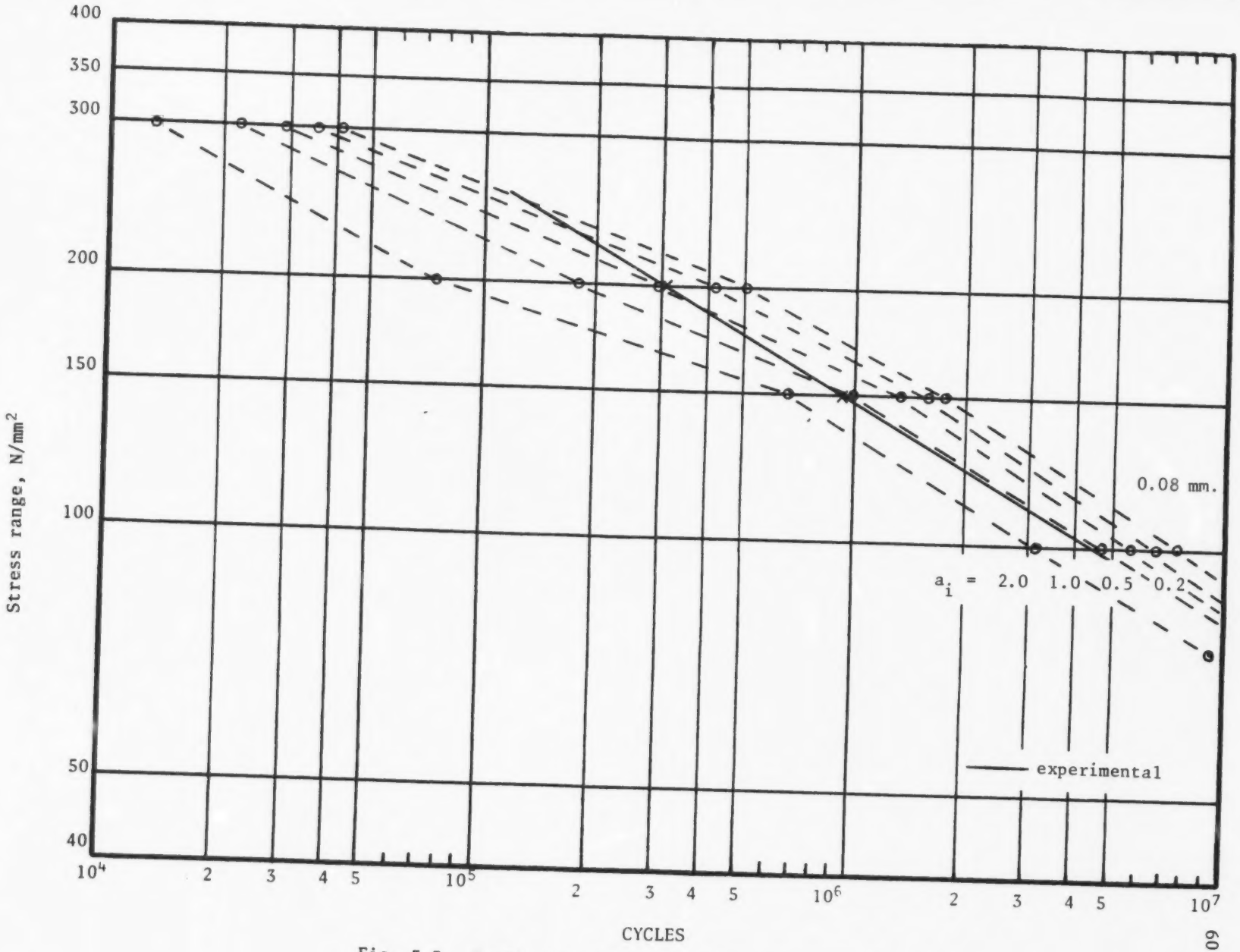

Fig. 3.5 - Prediction Results Showing Influence of Initial Crack Size: t = 16 mm

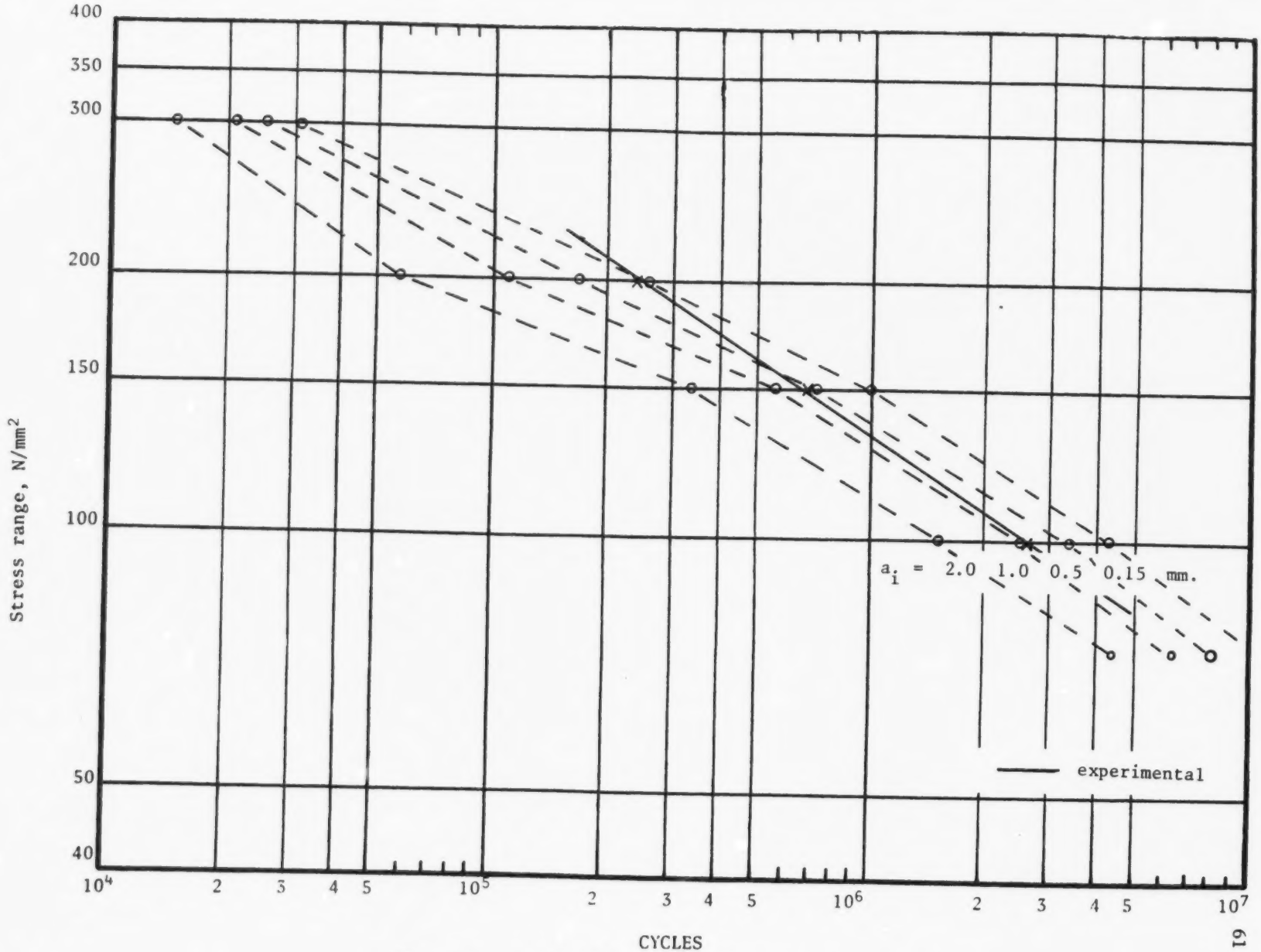

Fig. 3.6 - Prediction Results Showing Influence of Initial Crack Size: t = 26 mm

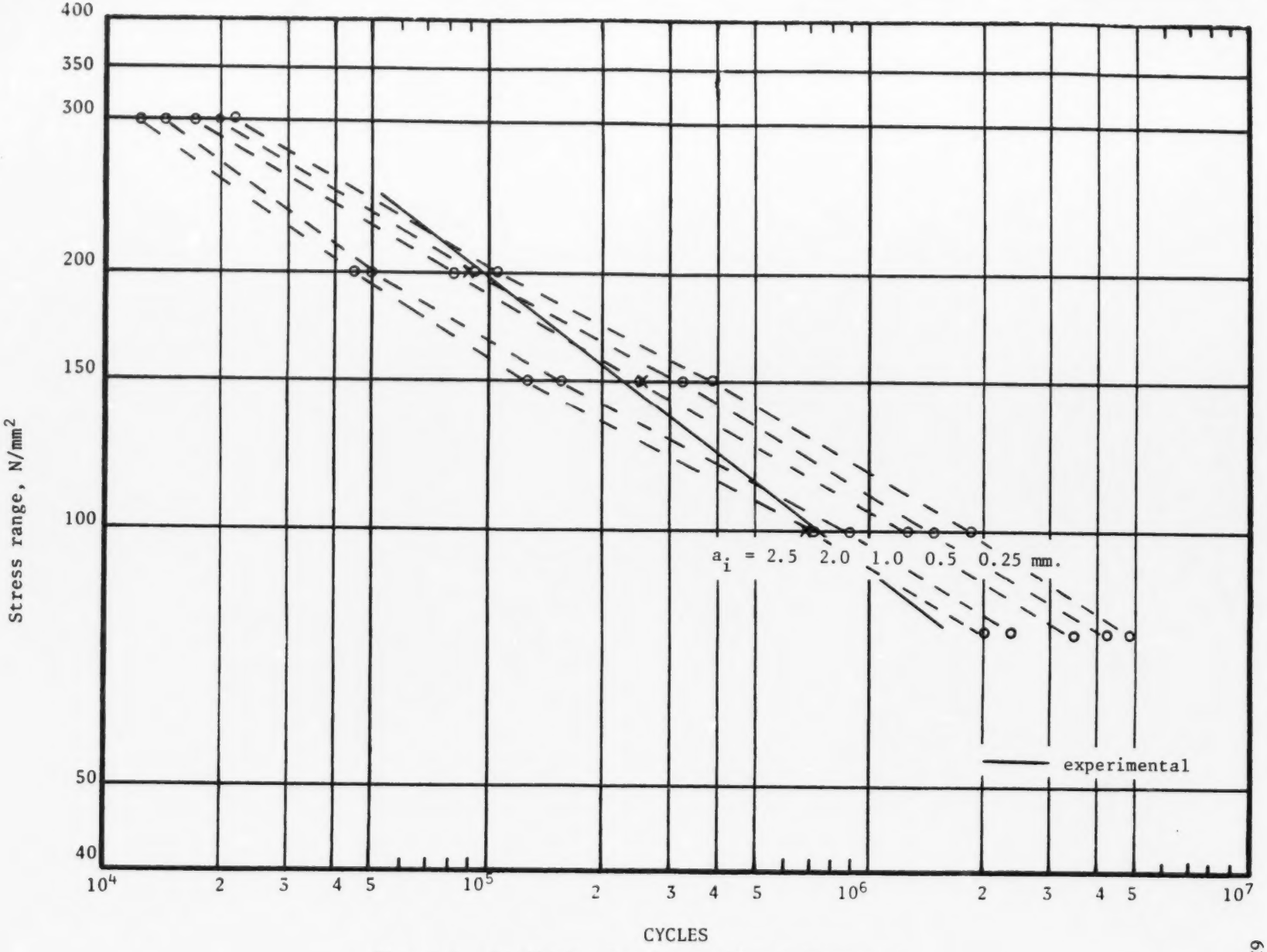

Fig. 3.7 - Prediction Results Showing Influence of Initial Crack Size: t = 52 mm

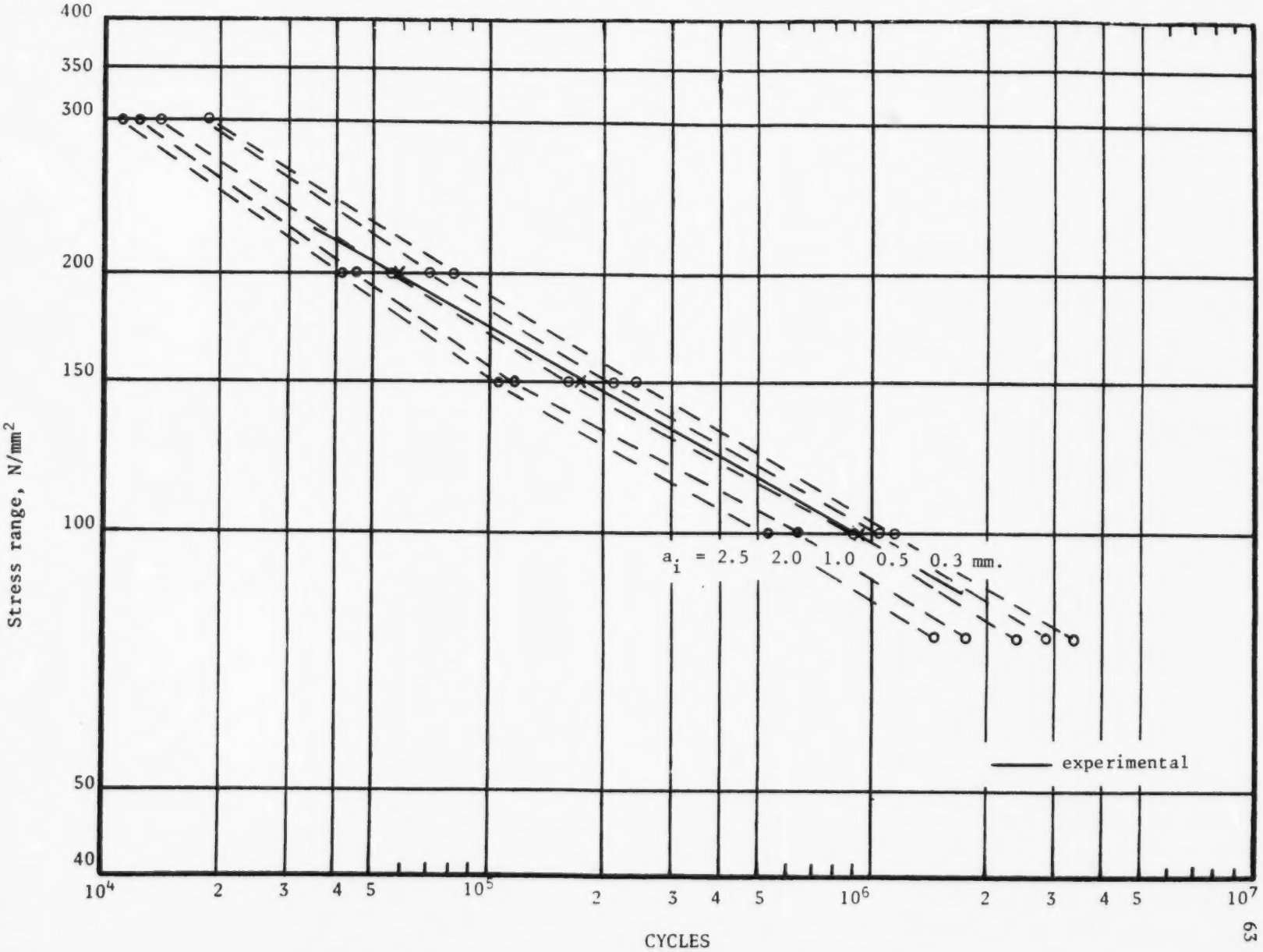

Fig. 3.8 - Prediction Results Showing Influence of Initial Crack Size: t = 78 mm

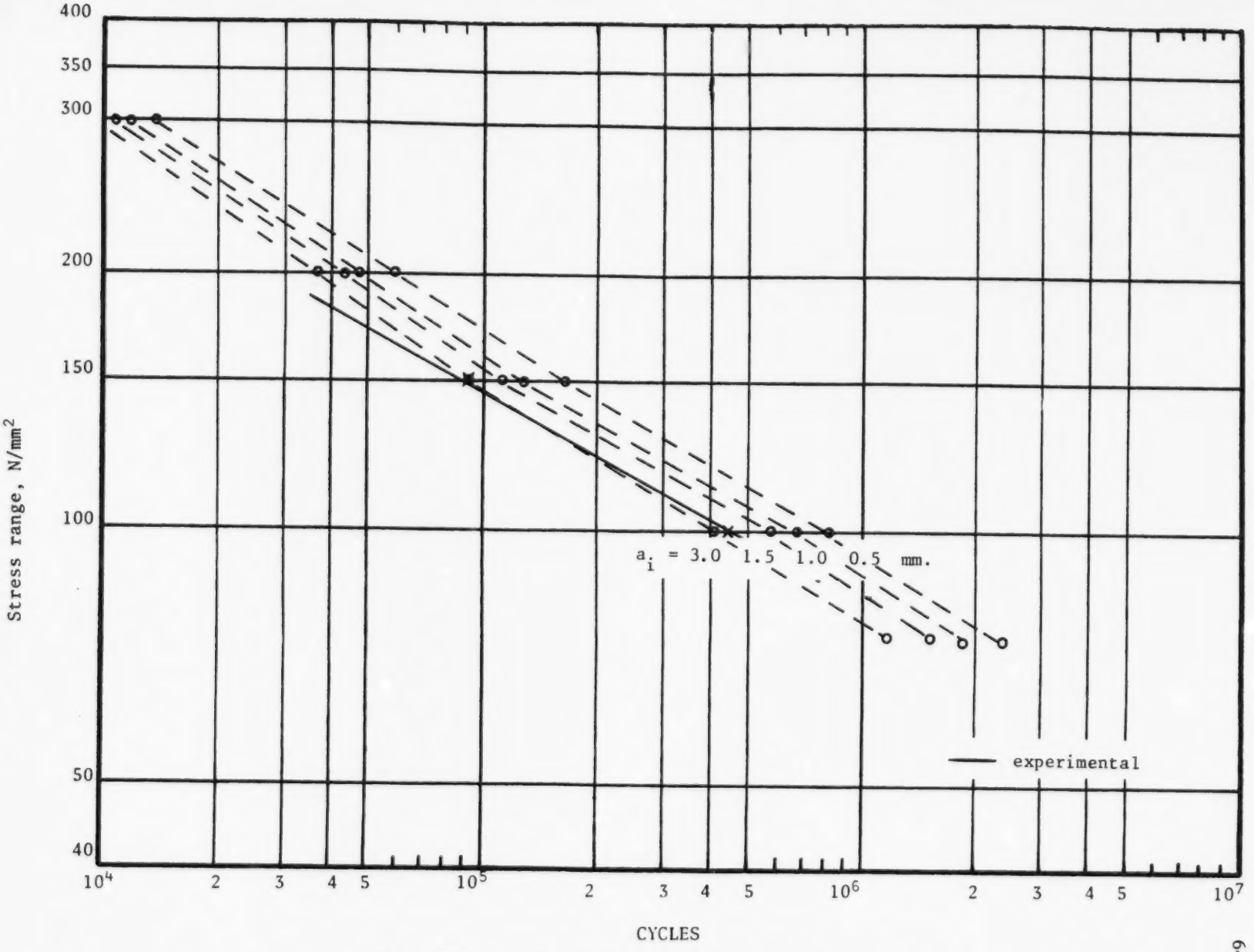

Fig. 3.9 - Prediction Results Showing Influence of Initial Crack Size: t = 103 mm

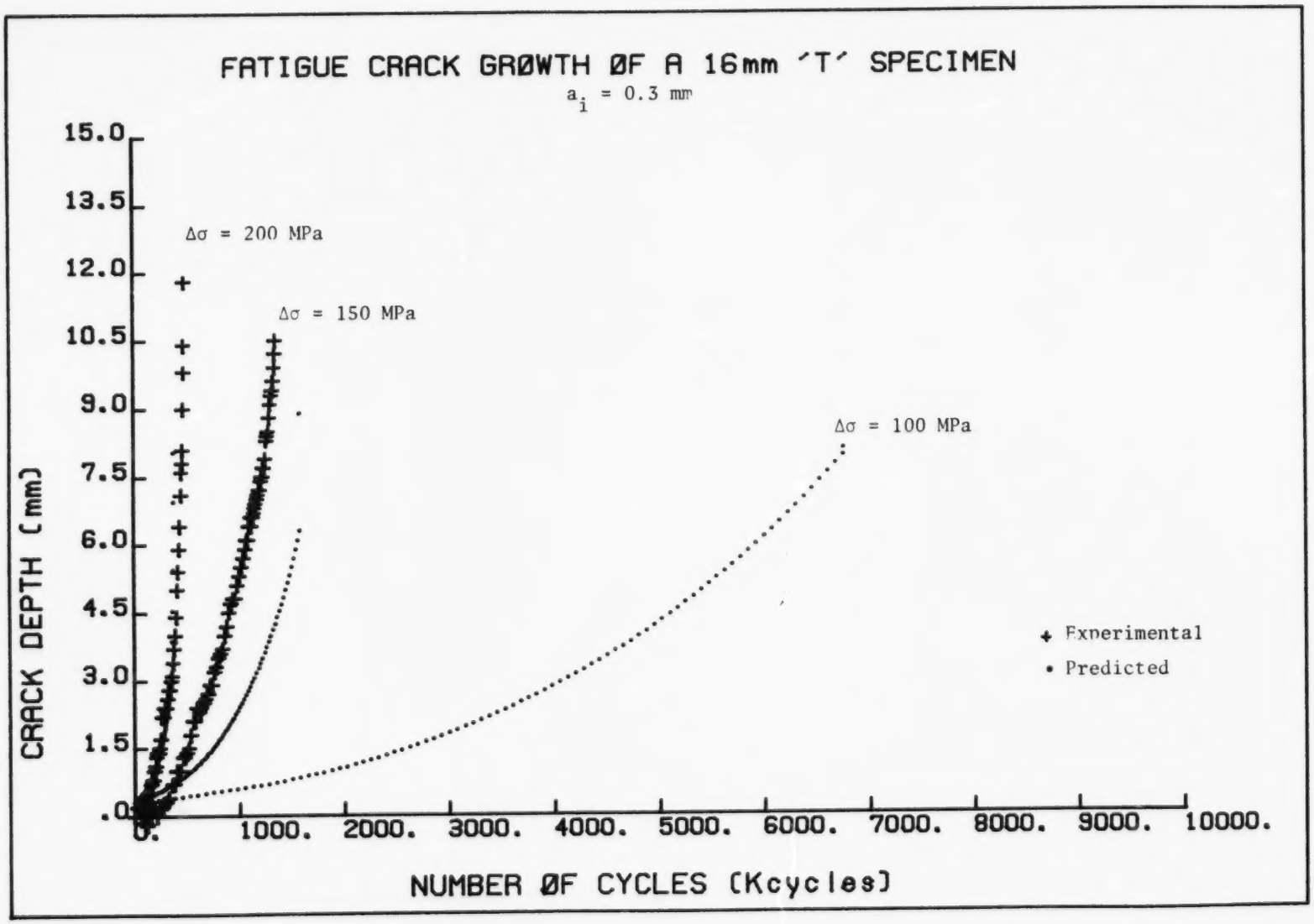
FATIGUE CRACK GRØWTH ØF A 16mm 'T' SPECIMEN
a_i = 0.3 mm
15.0
13.5
12.0
10.5
9.0
7.5
6.0
4.5
3.0
1.5
.0
CRACK DEPTH (mm)
Δσ = 200 MPa
Δσ = 150 MPa
Δσ = 100 MPa
+ Experimental
• Predicted
0.
1000.
2000.
3000.
4000.
5000.
6000.
7000.
8000.
9000.
10000.
NUMBER ØF CYCLES (Kcycles)

Fig. 3.10

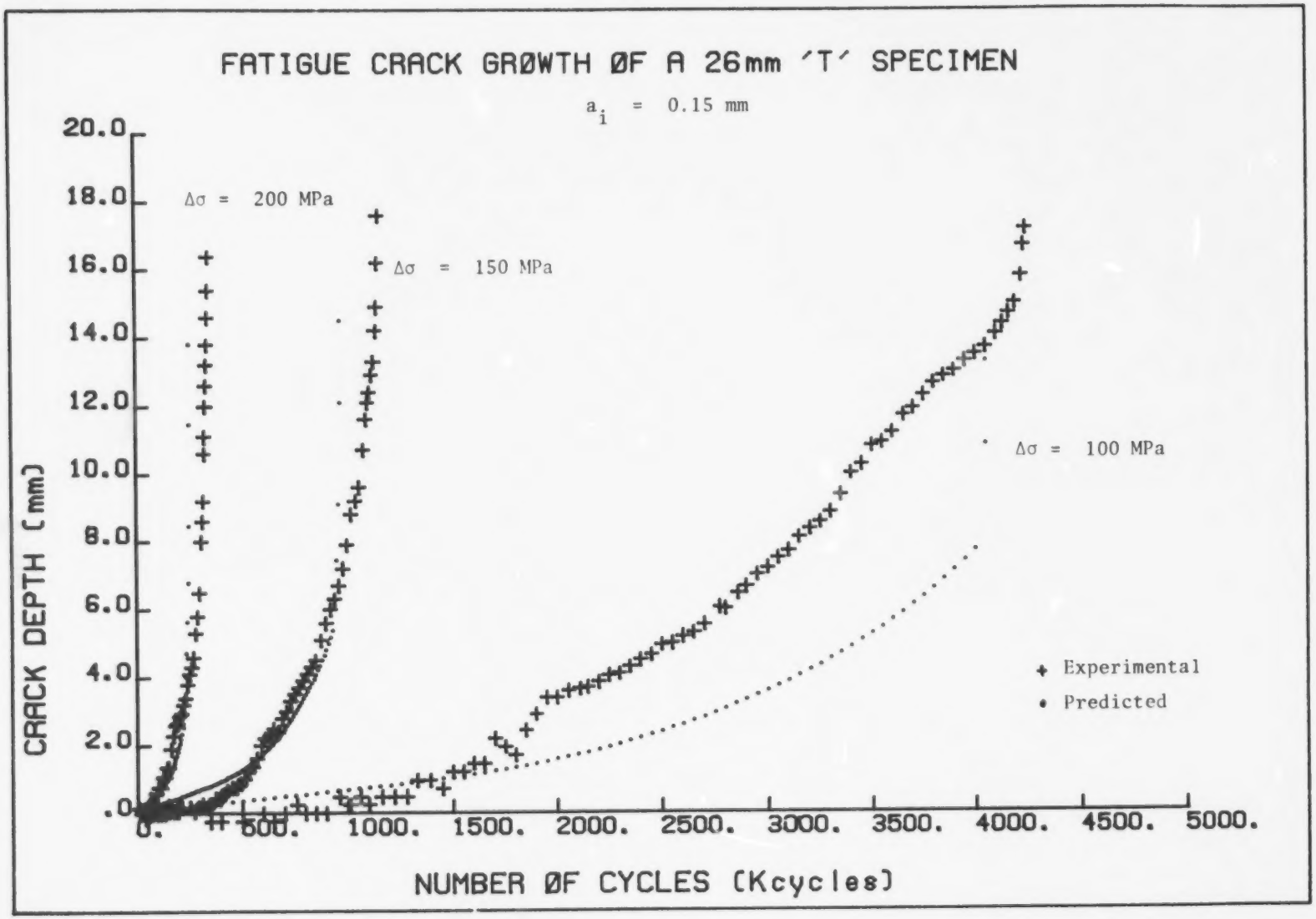
FATIGUE CRACK GRØWTH ØF A 26mm 'T' SPECIMEN
a_i = 0.15 mm
Δσ = 200 MPa
Δσ = 150 MPa
Δσ = 100 MPa
Experimental
Predicted
CRACK DEPTH (mm)
NUMBER ØF CYCLES (Kcycles)
20.0
18.0
16.0
14.0
12.0
10.0
8.0
6.0
4.0
2.0
.0
0.
500.
1000.
1500.
2000.
2500.
3000.
3500.
4000.
4500.
5000.

Fig. 3.11

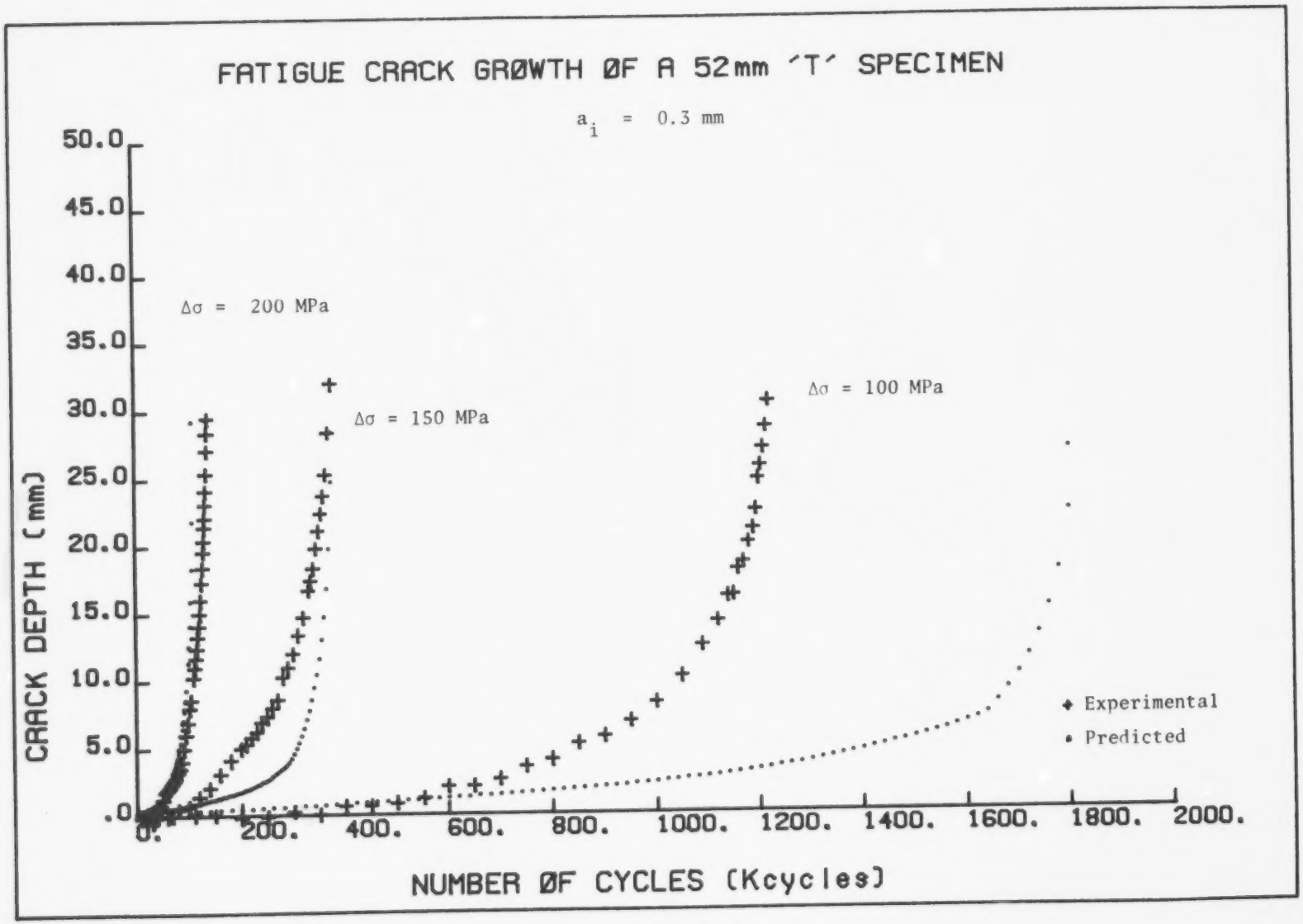
FATIGUE CRACK GRØWTH ØF A 52mm 'T' SPECIMEN
a_i = 0.3 mm
Δσ = 200 MPa
Δσ = 150 MPa
Δσ = 100 MPa
Experimental
Predicted
CRACK DEPTH (mm)
NUMBER ØF CYCLES (Kcycles)
50.0
45.0
40.0
35.0
30.0
25.0
20.0
15.0
10.0
5.0
.0
0.
200.
400.
600.
800.
1000.
1200.
1400.
1600.
1800.
2000.

Fig. 3.12

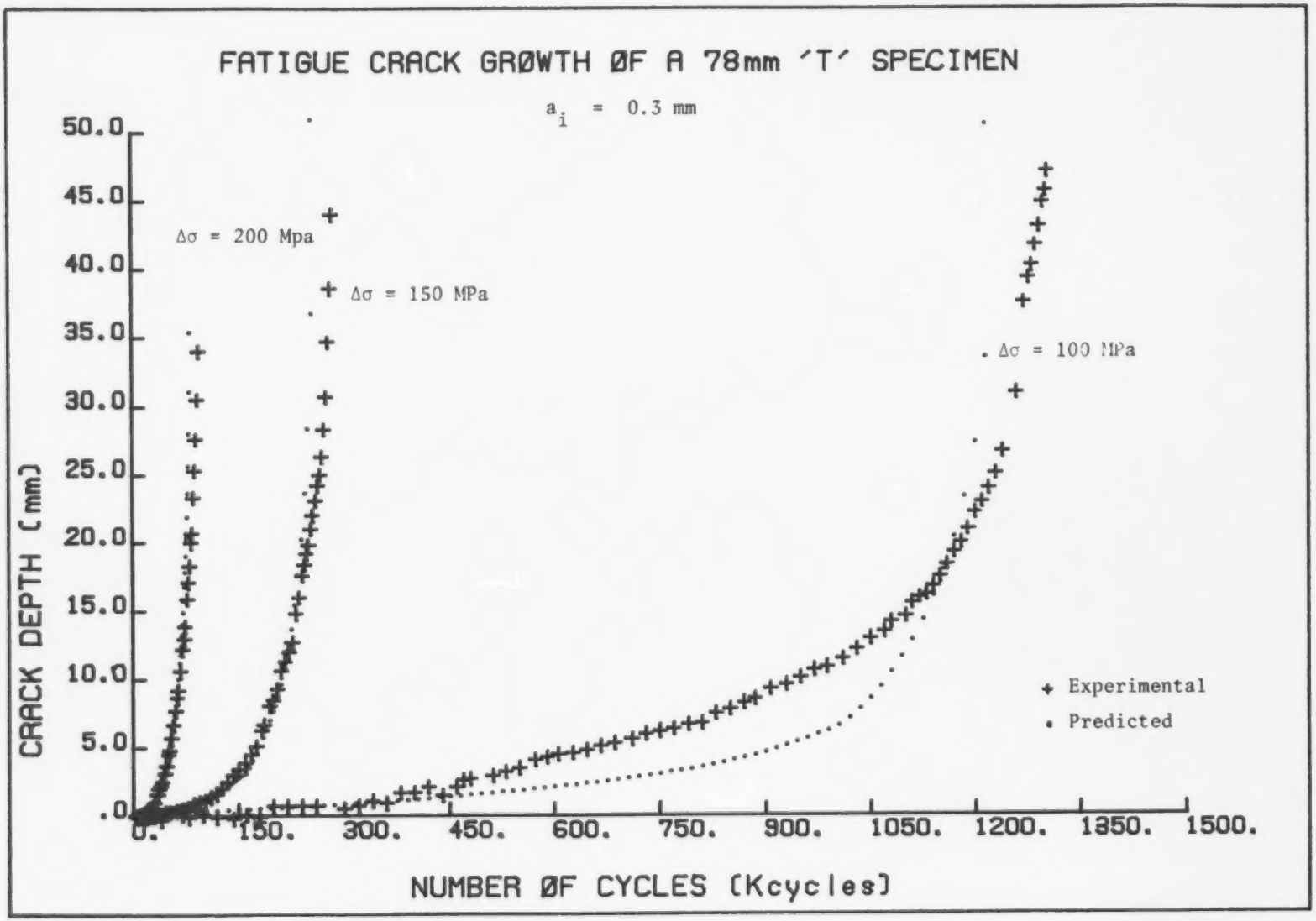
FATIGUE CRACK GRØWTH ØF A 78mm 'T' SPECIMEN
a_i = 0.3 mm
Δσ = 200 Mpa
Δσ = 150 MPa
Δσ = 100 MPa
Experimental
Predicted
CRACK DEPTH (mm)
50.0
45.0
40.0
35.0
30.0
25.0
20.0
15.0
10.0
5.0
.0
0.
150.
300.
450.
600.
750.
900.
1050.
1200.
1350.
1500.
NUMBER ØF CYCLES (Kcycles)

Fig. 3.13

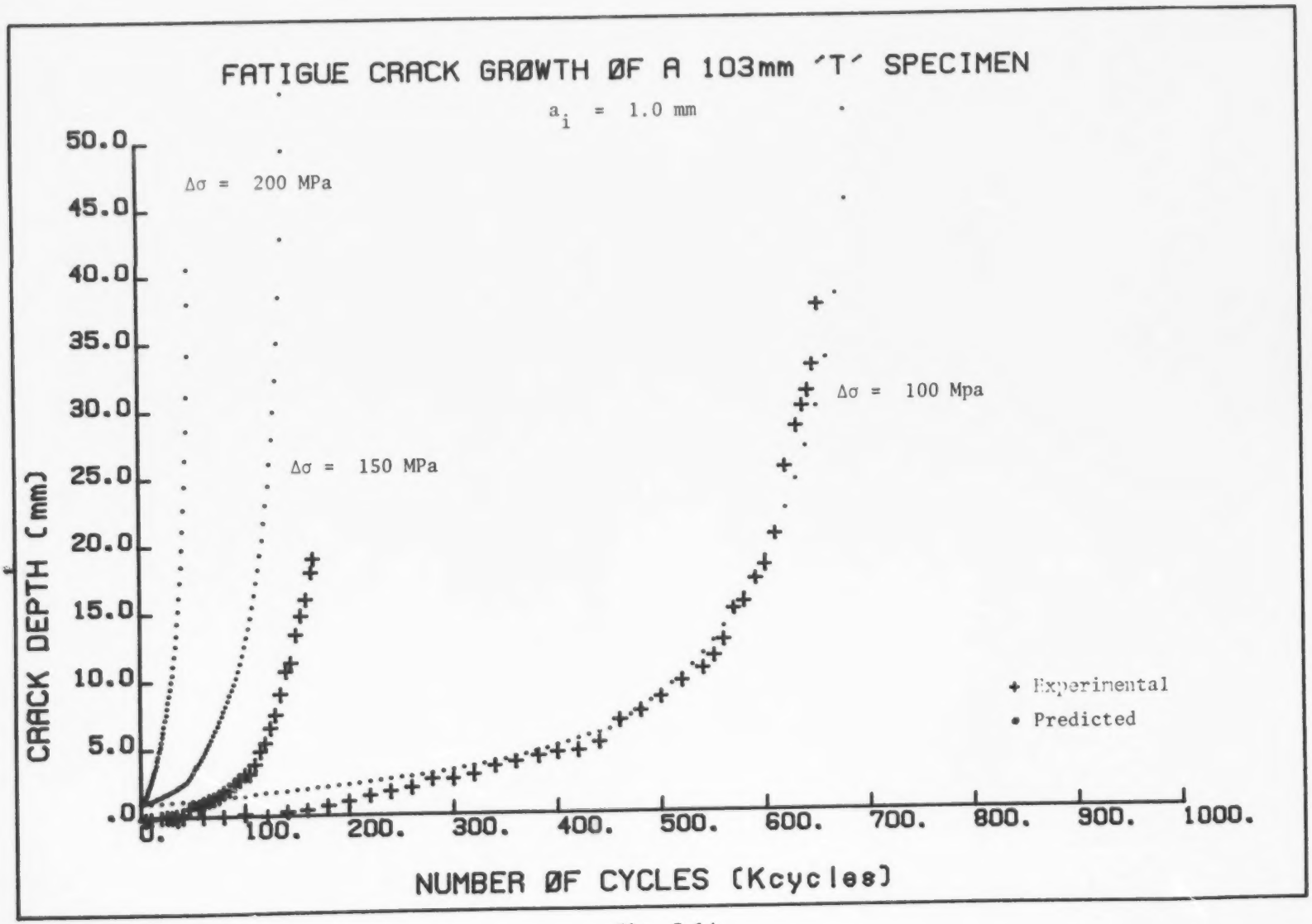
FATIGUE CRACK GRØWTH ØF A 103mm 'T' SPECIMEN
a_i = 1.0 mm
Δσ = 200 MPa
Δσ = 150 MPa
Δσ = 100 Mpa
+ Experimental
• Predicted
CRACK DEPTH (mm)
50.0
45.0
40.0
35.0
30.0
25.0
20.0
15.0
10.0
5.0
.0
0.
100.
200.
300.
400.
500.
600.
700.
800.
900.
1000.
NUMBER ØF CYCLES (Kcycles)

Fig. 3.14

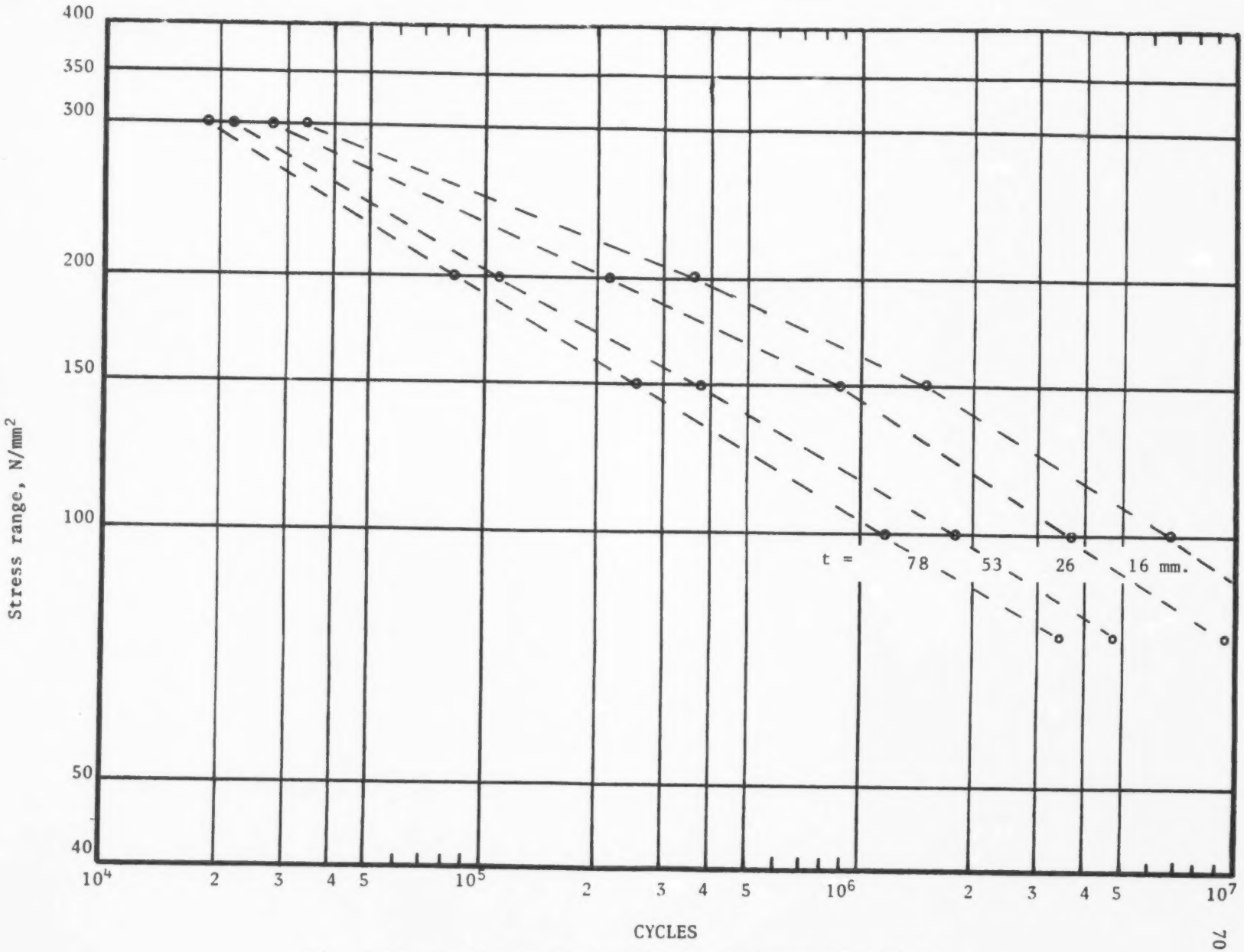

Fig. 3.15 - Prediction Results Showing Influence of Thickness
For an Initial Crack Size: $a_i = 0.3$

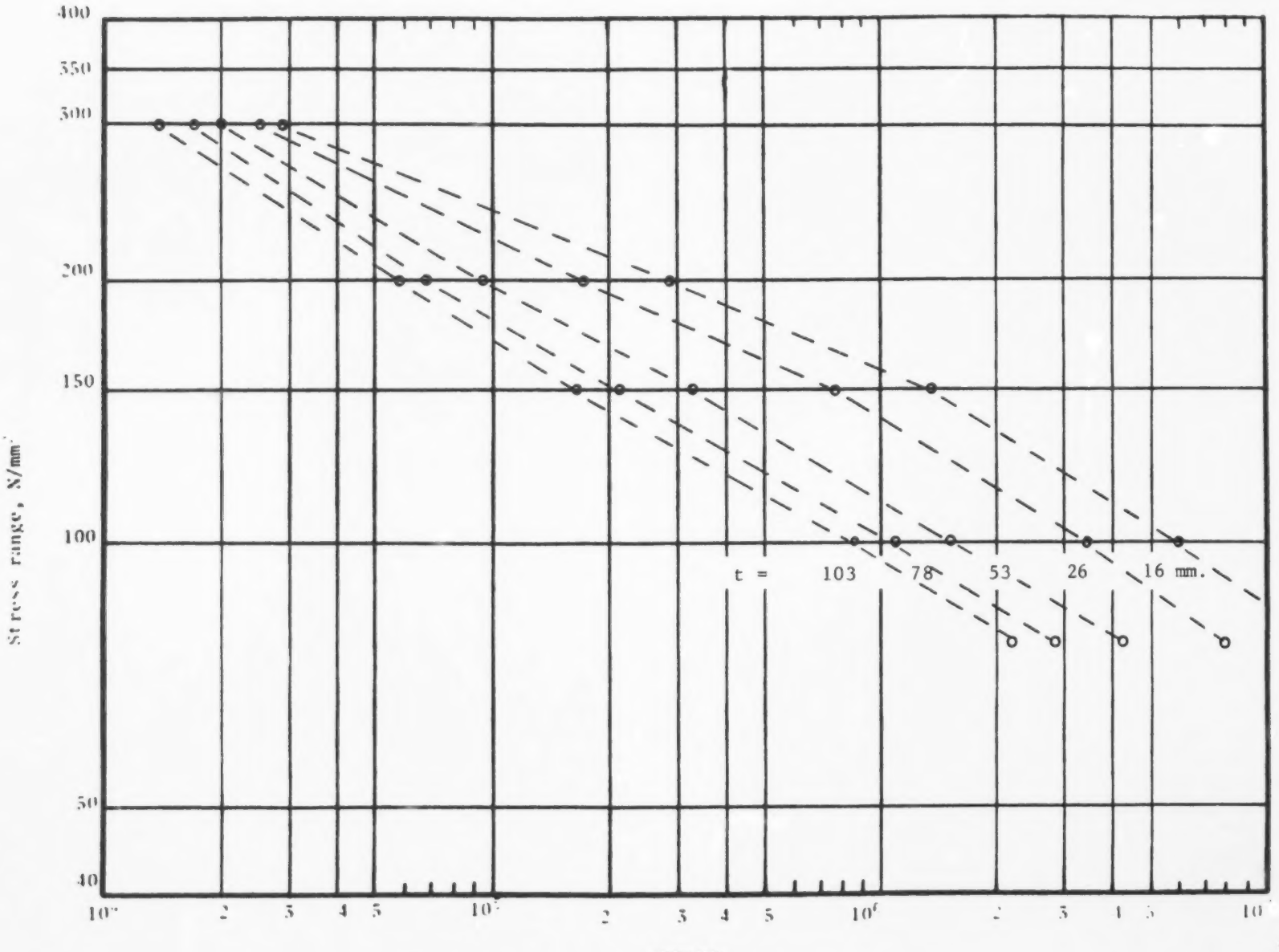

Fig. 3.16 - Prediction Results Showing Influence of Thickness
For an Initial Crack Size: $a_i = 0.5$

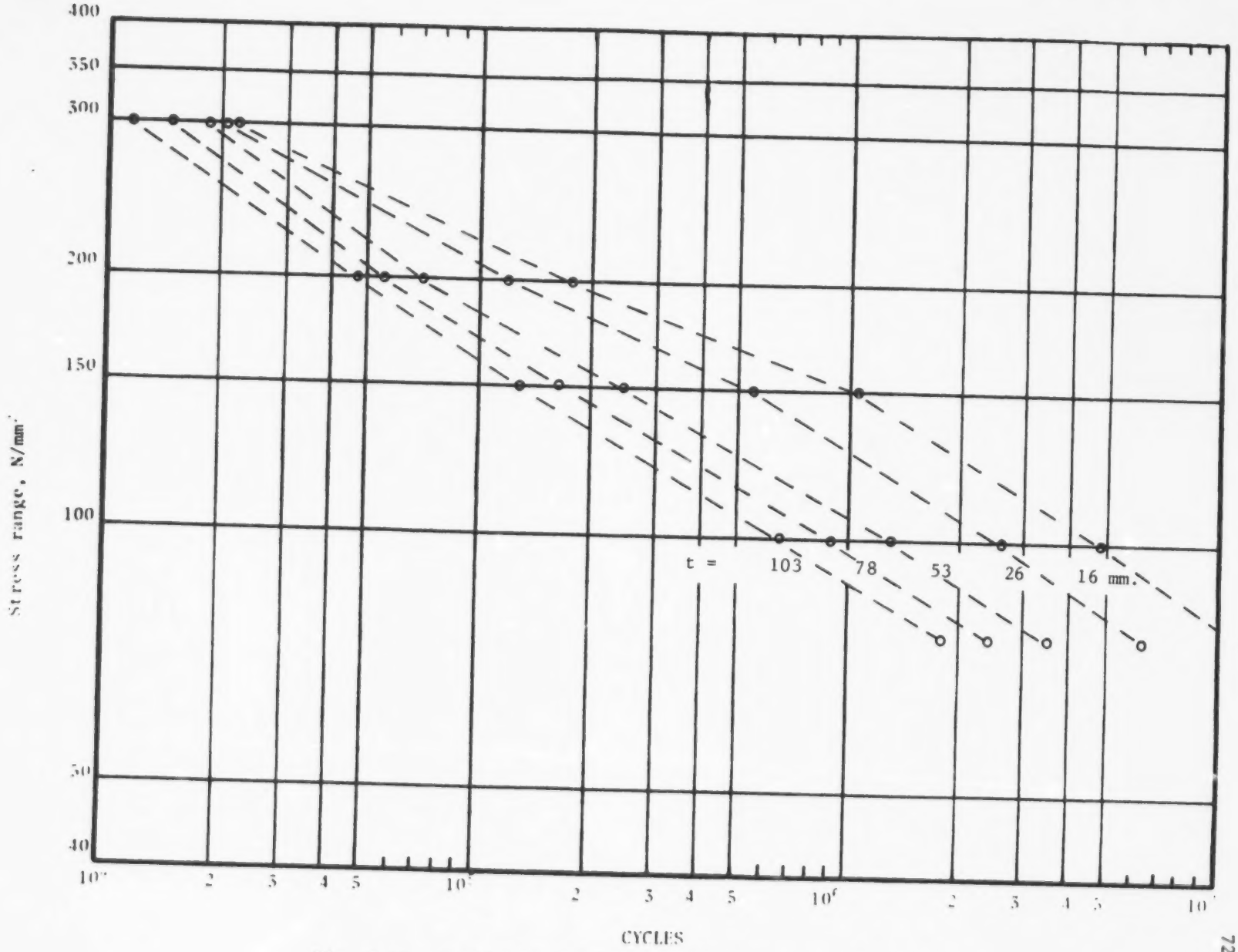

Fig. 3.17 - Prediction Results Showing Influence of Thickness For an Initial Crack Size: $a_i = 1.0$

CHAPTER IV

THE EFFECT OF SUPPORT SPAN ON SIF RESULTS

4.1 Introduction

In order to investigate the effect of support span, (dimension L in Figure 4.1), on the SIF data, the following study was carried out. It was decided to perform several finite element analyses and calculate the SIF for different spans. Due to cost considerations the work was performed using the 2-Dimensional finite element mesh described in the Phase I Report.

These analyses were carried out for shallow crack depths of a/t = 0.1, 0.03 and 0.015 and for three weld shapes of 30^{o}, 45^{o} and 70^{o}. The dimensions of the model are given in Figure 4.1. The distance x is defined as the distance from the crack plane to the support point. The load applied through the vertical member was adjusted so that a unit axial stress was applied at the crack plane for each span investigated

The results are presented in terms of M_k, a SIF magnification factor. Therefore, the stress intensity factor at the weld toe is obtained by multiplying the magnification factor by the stress intensity factor for the same size of crack in the plate when there is no weld present. i.e.,

$$K_{I\ weld} = M_k\ K_{I\ no\ weld}.$$

4.2 2-Dimensional Finite Element Results

The results from these studies are presented in tables 4.1 to 4.3 and plotted in Figures 4.2 to 4.4.

From the results presented for small crack sizes certain trends can be observed. It appears that the SIF does increase with decreasing span, however this effect only becomes significant when the distance from the crack to the support point, x, is less than 100 mm. It can also be seen that the effect of decreasing span has less effect on the SIF as the crack progresses through the thickness. No attempt will be made to explain the above effect; however, it is suggested that it may be due to the loading not being totally mode I at small values of span.

It can be assumed that similar results would be obtained if the above investigation had been carried out as a 3-dimensional study.

4.3 Significance of Span Effect on Present Work

In order to assess the effect of support span on present work it is necessary to consider the span of the support point on the finite element model used to obtain the stress intensity factors and to compare this with the span of the test specimens given in (9).

The stress intensity factors obtained using 3-dimensional finite elements were calculated from the model shown in Figure 2.2. In this case

the span was 600 mm and the distance x from the crack plane to the support point was 245 mm. In the experimental study described in (9) the spans are given in Figure 3.4, and the values of x varied from 130 mm for the 16 mm thick specimen to 257 mm for the 102 mm specimen. The weld angle in these tests was nominally 45^{o}.

Therefore, given the above information and the effect of span on SIF shown in section 4.2, it can be assumed that it is not necessary to make corrections to the SIF data used for the life prediction results presented for the "T" plate specimens.

Weld Angle	L (mm)	x (mm)	M_k	% Change
30^o	950	375	1.713	0
	750	275	1.722	0.5
	550	175	1.759	2.7
	300	50	2.122	23.9
45^o	950	375	1.930	0
	750	275	1.954	1.2
	550	175	2.018	4.6
	300	50	2.519	30.5
70^o	950	375	2.101	0
	750	275	2.134	1.6
	550	175	2.214	5.4
	300	50	2.876	36.9

Variation of M_k (2-D)
for a/t = 0.015

TABLE 4.1

Weld Angle	L (mm)	x (mm)	M_k	% Change
30^o	950	375	1.483	0
	750	275	1.498	1.0
	550	175	1.517	2.3
	300	50	1.645	10.9
45^o	950	375	1.606	0
	750	275	1.625	1.2
	550	175	1.662	3.5
	300	50	1.839	14.5
70^o	950	375	1.687	0
	750	275	1.712	1.5
	550	175	1.766	4.7
	300	50	1.980	17.4

Variation of M_k (2-D)
for a/t = 0.03

TABLE 4.2

Weld Angle	L (mm)	x (mm)	M_k	% Change
30^o	950	375	1.199	0
	750	275	1.208	0.8
	550	175	1.220	1.8
	300	50	1.300	8.4
45^o	950	375	1.214	0
	750	275	1.225	0.9
	550	175	1.242	2.3
	300	50	1.333	9.8
70^o	950	375	1.231	0
	750	275	1.241	0.8
	550	175	1.262	2.5
	300	50	1.359	10.4

Variation of M_k (2-D)
for a/t = 0.1

TABLE 4.3

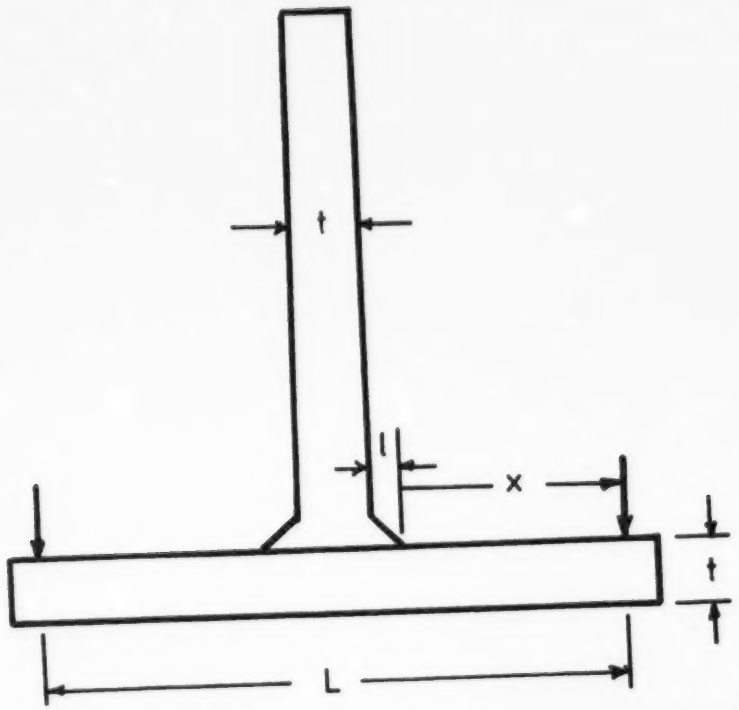

t = 100 mm
l = 50 mm

Fig. 4.1

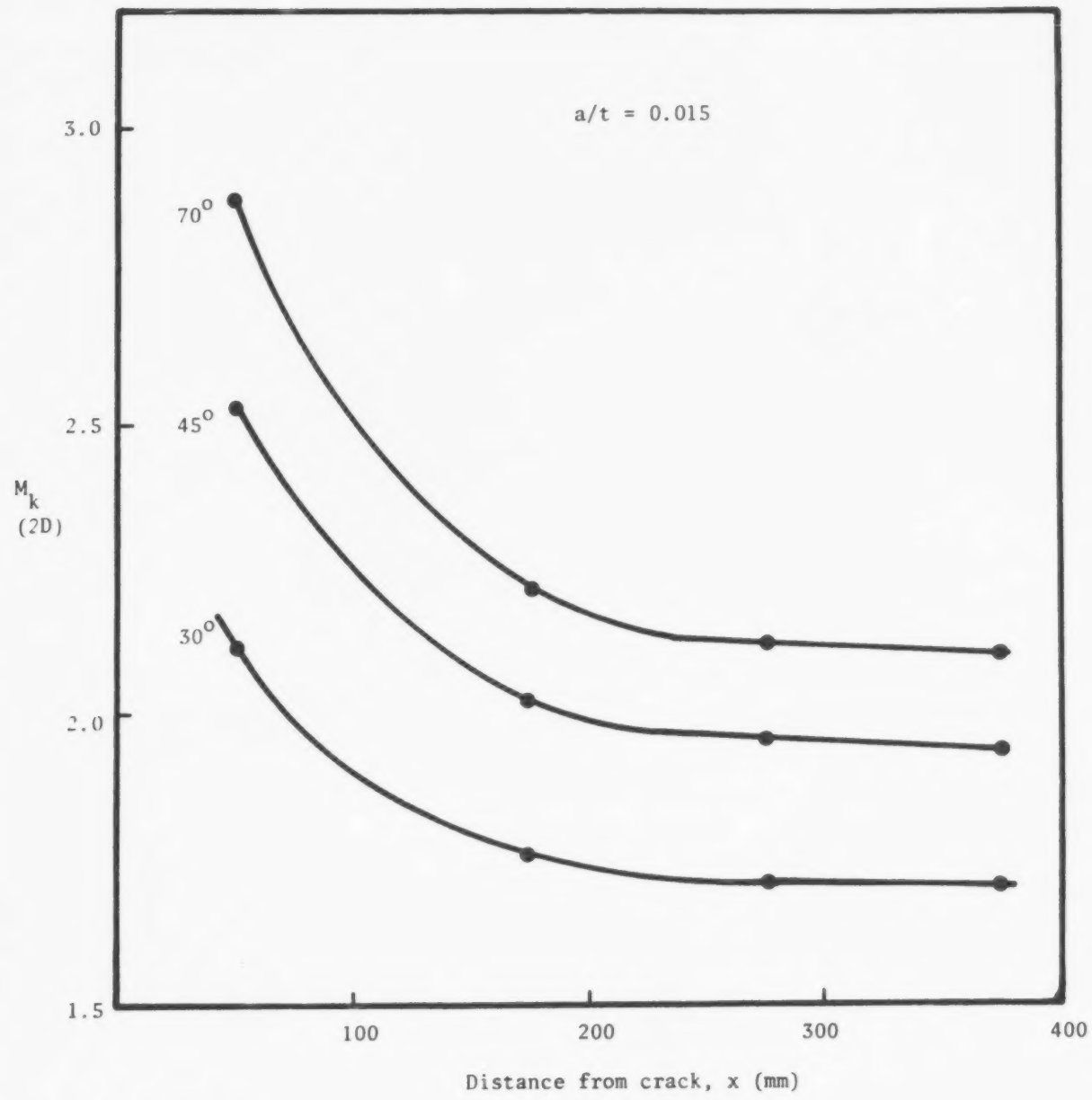

Variation of M_k (2-D) with span

FIGURE 4.2

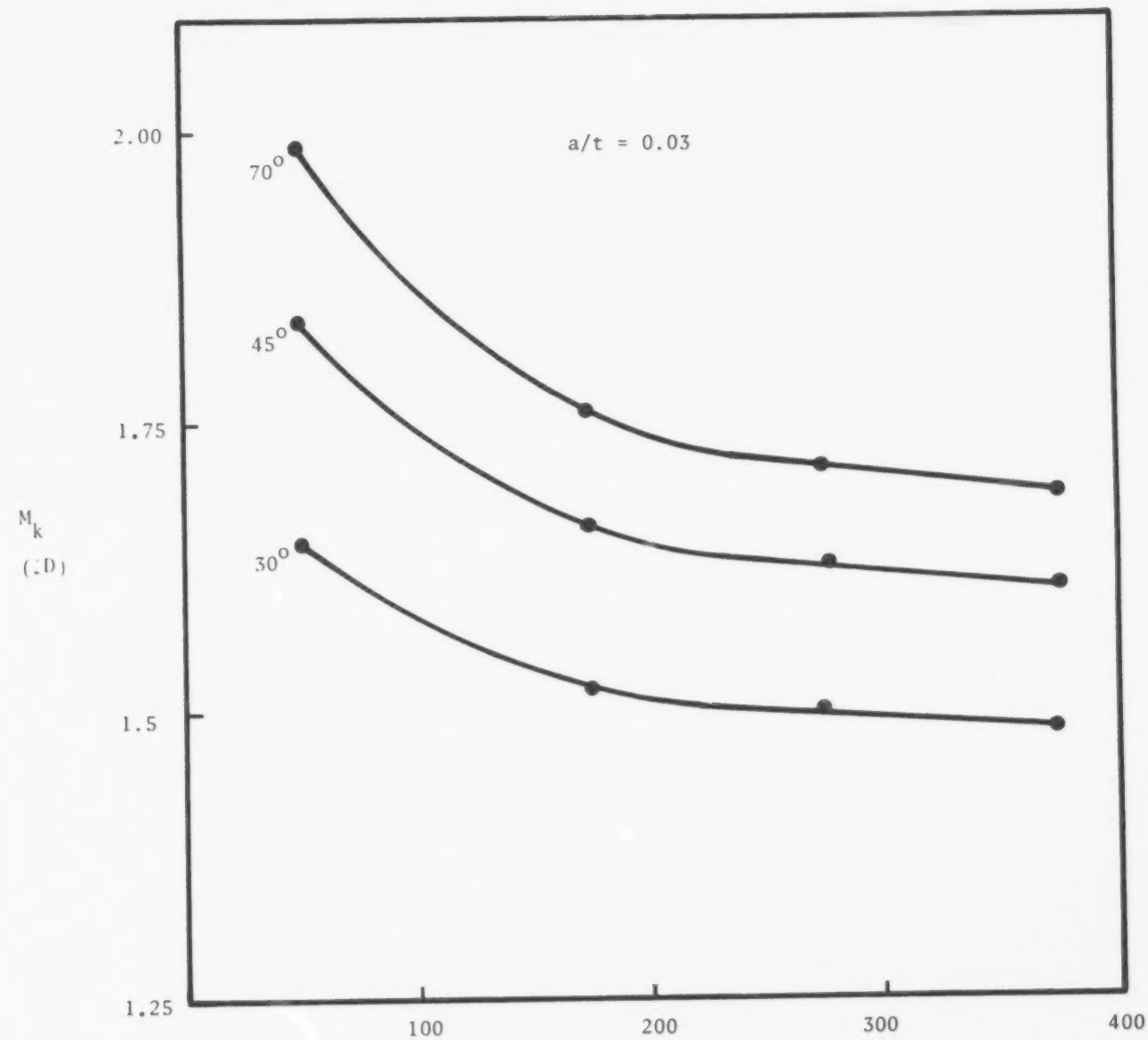

Variation of M_k (2-D) with span

FIGURE 4.3

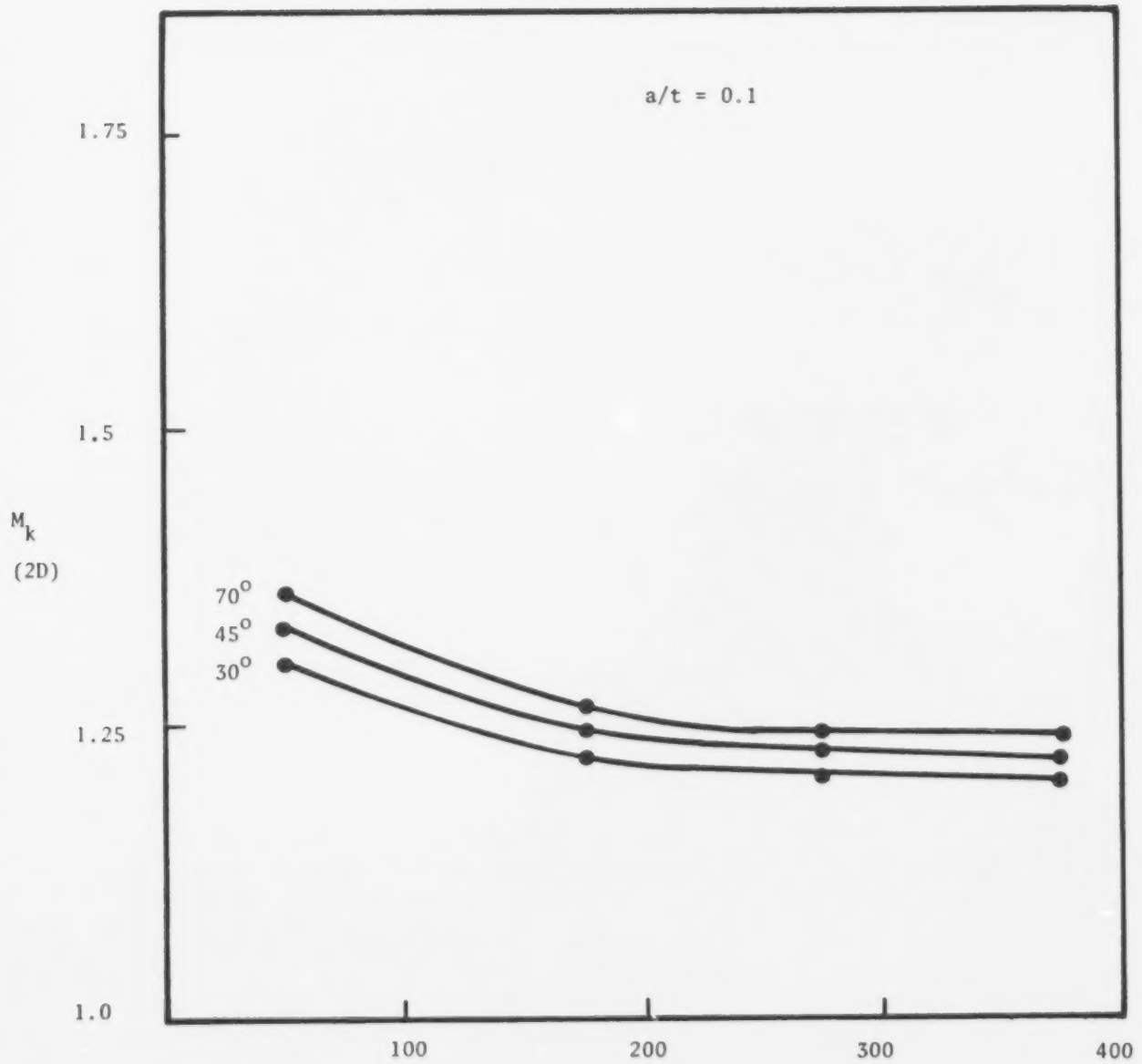

Variation of M_k (2-D) with span

FIGURE 4.4

CHAPTER V

CONCLUSIONS

1. The requirements of the contract work statement (Appendix A) have been met.

2. The general purpose finite element program ASAS has been used to expand the data base of 3-D finite element results for the SIF at weld toe defects with varying c/a and a/t ratios.

4. A computer program was written to predict the fatigue life of welded "T" plate joints. This program has the capabilities described in section 3.2 of this report.

5. The life prediction program has a prescribed shape development capability so that multiple crack growth and coalescence can be simulated.

6. An investigation was carried out to study the effect of initial crack size on the predicted life of welded "T" plate specimens. These results are presented in tabular and S-N diagram form.

7. The predicted fatigue life of the "T" plate specimens compared favourable with the published experimental results.

8. A 2-D finite element study was performed to investigate the effect of support span on the SIFs obtained.

9. It was found that for the geometries and loading spans considered in this work no correction to the SIF values need be applied.

REFERENCES

1. R. Bell and J. Kirkhope, "Determination of Stress Intensity Factors for Weld Toe Defects" (D.S.S. Contract OSU82-00233, Faculty of Engineering, Carleton University, Ottawa, 1984).

2. R. S. Barsoum, "On the Use of Isoparametric Finite Elements in Linear Fracture Mechanics", (Int. J. Numer. Methods in Eng. 10-1, pp. 25-37, 1976)

3. J. C. Newman and I. S. Raju, "An Empirical Stress Intensity Factor Equation for a Surface Crack", (Engineering Fracture Mechanics, Vol. 15, No. 1-2, pp. 185-192, 1981).

4. W. S. Burton, G. B. Sinclair, J. S. Solecki and J. L. Swedlow, "On the Implications for LEFM of the Three-Dimensional Aspects in Some Crack/Surface Intersection Problems", (Int. J. of Fracture Mechanics, Vol. 25, pp. 3-32, 1984).

5. O. Vosikovsky, "Effect of Mechanical and Environmental Variables on Fatigue Crack Growth Rates in Steels", (Canadian Metallurgical Quarterly, Vol. 19, No. 1, pp. 87-97, 1980).

6. T. R. Gurney and G. O. Johnston, "A Revised Analysis of the Influence of Toe Defects on the Fatigue Strength of Transverse Non-Load-Carrying Fillet Welds", (Welding Research International 9-3, pp. 43-79, 1979).

7. G. R. Irwin, "The Crack Extension Force for a Part - Through Crack in a Plate", (Trans. ASME, J. of Appl. Mech. Vol. 29, No. 4, 1962).

8. H. G. Morgan, "The Effect of Section Thickness on the Fatigue Performance of Simple Welded Joints", (Report NO-R-941 (S), UKAEA, HMSO London, Oct. 1983).

9. O. Vosikovsky, R. Bell, D. J. Burns and U. H. Mohaupt, "Fracture Mechanics Assessment of Fatigue Life of Welded Plate T-Joints, Including Thickness Effect", (Proc. 4th Int. BOSS Conf. pp. 453-464, Delft, 1985).

APPENDIX "A"

PHASE I

STATEMENT OF WORK

Background:

Economic design and safe operation of large off-shore platforms requires thorough understanding of fatigue and corrosion fatigue damage of welded joints. The evaluation of structural integrity and likely the future design is based on fracture mechanics predictions of fatigue crack growth from initial welding defects. For these predictions the knowledge of stress intensity factors for defects and cracks in weld is essential.

The determination of stress intensity factors for weld cracks will complement the CANMET research project on corrosion fatigue of welded joints for offshore structures.

Requirements:

To determine stress intensity factors for surface cracks in welded T joint using finite element analysis. To investigate the effects of weld shape and crack geometry on stress intensities

Work Statement:

Determine the stress intensity factor for cracks at the toe of a weld in T-joint.

1. 2 dimensional case

   a) obtain the SIF for crack depths a/B=0.01, 0.02, 0.05, 0.1, 0.3, 0.5, 0.7

   b) investigate the effect of weld shape on SIF for shallow cracks

2. 3 dimensional case

   a) obtain SIF for semi-elliptical cracks with aspect ratios $\frac{a}{c}$ = 1,0, 0.5, 0.25, with $\frac{a}{B}$ in rage 0.01 to 0.3 -

   b) investigate the effect of weld shape on SIF for shallow cracks.

APPENDIX "A.1"

ADDITION TO STATEMENT OF WORK

PHASE I

At Item 1 - Add the following:

c) Determine stress concentration and distribution of stresses at the weld toe for 45° and 60° welds, and for thicknesses15, 28, 53, 78 and 103mm.

d) Derive analytical expression for dependence of SIF on the depth of weld toe crack.

At Item 2 - Add the following:

c) Obtain SIF for 12 combinations of crack aspect ratios and crack depth. The selected combinations are to be agreed on with the Scientific Authority.

DSS FILE NO. 22ST.23440-2-9083/1
SERIAL NO. 0ST84-00125

APPENDIX "A"

STATEMENT OF WORK

PHASE II

Phase II - "Development of numerical methods for fatigue life calculation of welded joints"

1. Develop numerical method for calculation of fatigue crack growth life of welded T-joints using previously determined SIFs, and the following inputs:

   a) Fatigue crack growth rate curve - defined by Paris equation
      - with change in slope
      - with threshold

   b) initial defect depth and shape

   c) final crack depth

   d) natural or prescribed variation of crack shape (aspect ratio) with depth

   The method should be developed for constant amplitude loading with provisions for modifications to accept variable amplitude loading.

2. Calculate fatigue lives of T-joints with five geometries (t=16,28,52,78,102 mm) tested at CANMET, to verify the accuracy of predicted lives.

3. Complete FEM calculations of SIFs for the following six combinations of crack shape and depth:

$\frac{a}{c}$	$\frac{a}{t}$
1	0.01
0.5	0.01
	0.3
0.25	0.15
	0.30
	0.50

4. Evaluate the effect of span on SIF.

5. In addition to the research activity listed above in 1-4, the performer is required to attend an IIW Conference on the welding of tubular structures, Boston, July 16/17, 1984.